Ocean Engineering

Experimental investigation on the infragravity wave on different reef systems under irregular wave action

--Manuscript Draft--

Manuscript Number:	OE-D-20-02481R1
Article Type:	Full length article
Keywords:	Infragravity wave; Fringing reef; Platform reef; Shoreline; Wave set-up
Corresponding Author:	Bing Ren, Ph.D The State Key Laboratory of Coastal and offshore Engineering, Dalian University of Technology Dalian, Liaoning CHINA
First Author:	Gancheng Zhu, Ph.D. candidate
Order of Authors:	Gancheng Zhu, Ph.D. candidate
	Bing Ren, Ph.D
	Ping Dong, Ph.D.
	Guoyu Wang, Ph.D.
	Weidong Chen, Ph.D. candidate
Abstract:	This paper presents the results of a laboratory investigation into the role of infragravity motions in reef hydrodynamics over different reef systems. Laboratory experiments are performed with reef profiles of a platform reef and a fringing reef under irregular wave conditions. The propagation and the distribution of the infragravity wave are different over these two reef systems. Analysis of the measured time histories of water surface elevation shows that shorter sea-swell (SS) waves, longer infragravity (IG) wave and mean water level on the reef flat are significantly larger in the fringing reef system. The IG wave height can be up to three times larger on the fringing reef than that on the platform reef. This marked increase of the IG wave is considered to be due to: (1) the superposition of incoming IG wave and reflected IG wave from shoreline; (2) more violent wave breaking in the surf zone that may enhance the transfer of wave energy from the frequency band of the shorter wave to IG wave. In this experiment, the wave breaking mechanism controls the relationship between IG wave height and water depth.

28 October 2020

Atilla Incecik
Editor
Ocean Engineering

Dear Professor Incecik:

I, along with my co-authors, would like to ask you to consider the attached manuscript entitled “Experimental investigation on the infragravity wave on different reef systems under irregular wave action” for publication in Ocean Engineering as an original article.

The manuscript consists of 18 pages of text, two tables and 9 figures. Its content mainly focuses on the laboratory investigation on the role of infragravity motions in the wave runup process on different reef systems. The experiment is carried out in the state key laboratory of coastal and offshore engineering in Dalian University of Technology in China. We believe that the findings of this study are relevant to the scope of your journal and will be of interest to its readership.

This manuscript has not been published or presented elsewhere in part or in entirety, and is not under consideration by another journal. All the authors have approved the manuscript and agreed with submission to your esteemed journal. There are no conflicts of interest to declare. My professional background includes a professorship at the Dalian University of Technology in China and a Ph.D. in Coastal Engineering.

Thank you very much for your attention and consideration.

Yours sincerely,
Prof. Bing Ren
The State Key Laboratory of Coastal and Offshore Engineering
Dalian University of Technology
Dalian, China, 116024
Tel.:+86 411 84706436
Fax: +86 411 84708526
Email: bren@dlut.edu.cn

Highlights

- A laboratory experiment is conducted to investigate the role of infragravity motions over different reef systems.
- The propagation and distribution of the infragravity wave on the reef flat are investigated based on the test results.
- Appreciable increase of the infragravity wave on the fringing reef is discussed to show the influences of the reef-fringed shoreline and wave breaking.
- Complex relationships between the infragravity wave and water depth are discussed and compared with previous studies

Declaration of interests

☒ The authors declare that they have no known competing financial interests or personal relationships that could have appeared to influence the work reported in this paper.

☐The authors declare the following financial interests/personal relationships which may be considered as potential competing interests:

CRediT authorship contribution statement

Gancheng Zhu: Investigation, Methodology, Writing - original draft, Formal analysis. **Bing Ren**: Validation, Methodology, Funding acquisition, Supervision, Writing - review & editing. **Dong Ping**: Supervision, Writing - review & editing, Formal analysis. **Guoyu Wang**: Writing - review & editing, Formal analysis. **Weidong Chen**: Formal analysis.

The authors would like to thank all reviewers for their constructive comments and suggestions. The point-by-point responses to all comments are given below. The parts in italic are the reviewer's comments, which are followed by our responses in blue. All main revisions are highlighted in the revised manuscript to enable easy identification.

Reviewer 1:

This paper presents the results of a laboratory investigation into the role of infragravity motions in reef hydrodynamics over different reef systems. However, there is no new finding. It is not suitable for this journal. More works should be done. The reasons for rejection are as followed.

1) *Many results are repeatable with other papers, such as in line 175, the finding is same as Baldock et al., 2012; Contardo and Symonds, 2013, in line 236 the finding is same as Zhu et al., 2018.*

Response:

The authors have to disagree with the reviewer's assertion that "there is no new finding" in this work. Some results including the specific line cited by the reviewer are included to demonstrate the consistencies of the experimental results with that of the previous experiments but these are not claimed as new findings.

The specific and substantive new findings which we want to highlight in this work are:

1. Most field observations of coral reef show a proportional relationship between infragravity wave and the water depth on the reef flat. The bottom friction and reef resonance are regarded as responsible for this phenomenon. However, the potential influence of wave breakpoint mechanism on the IG wave on the coral reef was not explored in these field observations. Our experiment is designed to reveal the influence of wave breakpoint mechanism on the IG wave on the reef flat with different water depth, where the influence of the bottom friction is ignored. The experimental results show that the wave breaking mechanism controls an opposite relationship between the IG wave height and the water depth to the field observations. Therefore, when water depth increases, the IG wave heights are influenced by different mechanisms which act counter to each other.
2. By comparing the experimental data of the platform reef and fringing reef systems under the same condition, we find that the larger IG wave height for the fringing

reef is not only the contribution of the wave reflection from the shoreline, but also the change of the wave breaking around the reef edge.

3. The effect of the incoming wave period on the IG wave height on the platform reef is discussed in our manuscript.
4. Also the phenomenon that IG wave height decreases rapidly around the reef edge on the platform reef flat is discussed in this manuscript.

The comparisons of IG wave between our experiment and previous studies include field observations and laboratory experiments are added in Section 5 in revised manuscript.

2) Some results are obvious. Of course, the IG will higher on the fringing reef, but the main reason is that water is blocked by the shoreline, which will lead to higher wave setup. Can this kind of setup be considered as IG? It should be discussed.

Response:

The mean water level on the reef flat is composed of two parts: (1) average wave set-up: the rise of water level averaged on the whole acquisition time; (2) IG wave: the oscillation of the wave set-up averaged on the SS wave periods.

We agree with the reviewer that on the fringing reef, the water is blocked by the shoreline, which leads to higher average wave set-up (as shown in Fig. 6a-Fig.6c). However, this kind of setup is not considered here as caused by IG wave. The setup that have been attributed to IG wave is the reflection of IG wave from the shoreline as discussed in section 5. The relevant discussion is added in the revised manuscript to make this point clear.

3) Another main finding of this paper is 'The IG wave height can be as three times larger on the fringing reef than that on the platform reef.' However this is a conclusion under a certain condition, including a vertical wall, 1:1 front slope, and 7.2m distance. Once the condition changes, it is also 3 times? It is not a common conclusion. It is suggested to author that more tests can be done to analyze the effects of distance, front slope on IG. Then a relationship can be obtained. It is more meaningful.

Response:

We agree with the reviewer that the relative size of the IG wave heights on the fringing reef and on the platform reef is observed under the specific setup of the experiment

such as a vertical wall, smooth surface and steep reef face. Must more tests will also be required to assess fully the effects of the distance and front slope on IG wave propagation to develop a more general relationship between the relative wave height and these controlling parameters. These points are added in the conclusion of revised manuscript.

4) Some minor details are missing as followed.

1. In line 101 'flat were finished with a smooth surface', what is the material of surface and roughness?

Response:

The surface of the reef model is made by smooth sand-cement grout. According to the quadratic drag law, the bed stresses induced by the wave-induced flow will lead to a decrease of wave set-up as:

$$\frac{d\bar{\eta}}{dx} = -\frac{C_f|U|U}{gh} \tag{1}$$

where U is depth-averaged current, h is the water depth on the reef flat. C_f is the quadratic drag coefficient, which indicates the roughness of the reef surface.

The C_f of the flat surface can be evaluated based on Eq (1). The depth-averaged current U roughly uses the point velocity measured by the velocity meter. C_f of the flat surface is ($O(0.001)$) and could be neglected.

2. In line 104 and 105, what's the instrument accuracy?

Response:

This point is taken. The measuring accuracy of the wave gauge is ± 0.1 mm. The measuring accuracy of the velocity meter is $\pm 0.5\%$ of the measured value.

The instrument accuracy is included in the revised manuscript.

3. In line 118, what's value of gama ?

Response:

This point is taken. Γ denotes the Hilbert transform. This operator applies a frequency independent phase shift of $\pi/2$.

$$\Gamma\big(f(t)\big) = \int f(t)\mathrm{e}^{-iwt}\mathrm{d}t \tag{2}$$

This explanation is included in the revised manuscript.

4. In line 133, how to synchronize wave and velocity signals when separating waves using Buckley's method ?

Response:

A data synchronous acquisition system is used to collect wave and velocity signals synchronously.

5. In line 157 Explain the reasons for effect of wave period on HIG ?

Response:

This point is taken. IG wave height has a positive correlation with the wave height variation of the incident wave group (Schäffer, 1993). For the irregular wave, the wave height variation of the wave group can be revealed by the wave groupiness of the incident wave. The increase of the wave period may lead to an increase in the wave groupiness (Karunarathna et al., 2005). Therefore, the wave groupiness of the incident wave increases with the increase of the significant wave period, which leads to an increase of the IG wave height.

This explanation is included in the revised manuscript.

6. In line179, no crest exists at the edge, why reflection happens?

Response:

The change of the water depth will induce wave reflection. When the outgoing waves propagate to the reef edge, the rapid change of the water depth between the horizontal reef flat and steep reef face can induce the wave reflection.

7. In line187, why does IG wave height decrease rapidly at G8?

Response:

This point is taken. This phenomenon is analyzed based on the observation of the wave breaking on the reef edge and the time series of the water surface for different water depths.

The photos of the wave overtopping on the reef edge are included in the revised manuscript. The relevant analysis results in added in paragraph two of Section 4.

8. In line233, Fig.8 should be Fig.9.

Response:

This is revised.

Reviewer 2:

General Comments: The authors present an experimental laboratory study of IG waves on reefs, discussed the generation and propagation of IG waves, and analysed the distribution of wave heights and wave setup on the reef flat. They considered a range of incident wave conditions; investigated two different reef systems (fringing and platform reefs) and discussed the differences between the two systems. The topic is of great interest. Overall, I think the paper is well structured, has an appropriate length, and the presented discussion of the experiment results is suitable. However, I believe the manuscript needs to be improved in the following areas:

- *Over the past decade, a number of studies investigated the subject of IG waves on reefs (some already cited in the manuscript; and few others which I listed in my review comments). However, except for a few lines (L#219-222), the authors did not provide any comparison between data and conclusions from the present experiment and those of the previous studies. I suggest a revision of Sections 3-5 to include a comparison (ideally quantitative) with previous studies, especially previous laboratory studies. I believe this would greatly enhance this paper.*

  Response:

  We agree with this comment completely. Field observations and laboratory experiments are compared in Table A1. The IG wave heights measured in Nwogu and Demirbilek's (2010) and Yao et al.'s (2020) laboratory experiment results are also reanalyzed in dimensionless form and shown in Fig. 11.

  Detailed discussion and comparison are added in Section 4 and 5 in the revised manuscript.

- *The language and the structure of sentences need to be significantly improved. Throughout the manuscript, there is redundancy in most sentences. I listed some instances in my review comments, and also provided rewording suggestions. However, I strongly suggest that the authors do a thorough revision of the entire manuscript for language and grammar issues.*

  Response:

The language and the structure of sentences are checked and reworded in the revised manuscript.

On this basis, most of my comments below are of editorial nature. With some minor modifications, I expect this paper would become a good addition to Ocean Engineering.

Specific Comments:

Line 17-18:

Consider rewording: "Measurements were made of water surface elevation and flow velocity at..."

Suggestion: "Water surface elevation and flow velocity were measured at ..."

Response:

This is reworded in the revised manuscript.

Line 19-21:

Consider rewording: "Analysis of the measured time histories of surface elevation over the reef face and flats shows that the fringing reef has appreciable increase in both shorter sea-swell (SS) waves, and longer infragravity (IG) waves as well as the mean water level on the reef flat"

Suggestion: "Analysis of the measured time histories of water surface elevation shows that shorter sea-swell (SS) waves, longer infragravity (IG) waves and mean water level on the reef flat are significantly larger in the fringing reef system."

Response:

This is reworded in the revised manuscript.

Line 22:

Consider rewording: "as three times larger ..."

Suggestion: "up to three times larger ..."

Response:

This is reworded in the revised manuscript.

Line 28:

Consider rewording this, plus removing redundancies:

"Million people in the world live in coastal areas adjacent to or near coral reefs ..."

Suggestion: "Millions of people worldwide live in coastal areas near coral reefs …"

Response:

This is reworded in the revised manuscript.

Line 29-33

Consider simplifying or breaking this long sentence:

"However, due to climate change and the degradation of coral reefs due to coastal development either for coastal residents or for the growing coastal tourism industry many coral reef-lined coasts are becoming increasingly vulnerable to wave-driven marine flooding resulting increased damage to coastal communities."

Suggestion:

"Reef-lined coasts, however, are becoming increasingly vulnerable to wave-driven flooding as a result of climate change and the reef degradation caused by coastal developments for residents and the growing tourism industry."

Response:

This is simplified in the revised manuscript.

Line 35:

Consider removing "that of waves on"

Response:

This is revised.

Line 39-41:

Here, when discussing the propagation and dissipation of short-wave energy on reefs, I suggest citing some of the existing studies in that area. Baldock et al (2020) is a recent one on the subject. References therein are also useful.

- *Baldock, E., Shabani, B., Callaghan, D., Zhifang, H., Mumby, P. (2020), "Two-dimensional modelling of wave dynamics and wave forces on fringing coral reefs", Coastal Engineering, 155, 103594.*

Response:

Studies on the dissipation of short-wave energy are added in the revised manuscript now.

Line 43-47:

When discussing IG waves on reefs:

Over the past decade or so, a few other studies (not cited in the manuscript) also investigated this subject. Below are some examples which include laboratory, field, and numerical studies (or a combination of them):

- *Nwogu, O., and Demirbilek, Z. (2010) "Infragravity wave motions and runup over shallow fringing reefs", J. Waterw. Port Coastal Ocean Eng., 136, 295–305.*
- *Van Dongeren, A., Lowe, R., Pomeroy, A., Trang, D., Roelvink, J., Symonds, G., and Ranasinghe, R. (2013) "Numerical modeling of low-frequency wave dynamics over a fringing coral reef." Coastal Eng., 73: 178–190.*
- *Pomeroy, A., Van Dongeren, A., Lowe, R., van Thiel de Vries, J. and Rovelvink, J. (2012) "Low frequency wave resonance in fringing reef environments", Coastal Eng. Proc., 1(33), 1595–160.*
- *Pequignet, A., Becker, J., and Merrifield, M. (2014) "Energy transfer between wind waves and low-frequency oscillations on a fringing reef, Ipan, Guam", J. Geophys. Res. Oceans, 119, 6709–6724.*
- *Beetham, E., Kench, P., O'Callaghan, J., and Popinet, S. (2016), "Wave transformation and shoreline water level on Funafuti Atoll, Tuvalu", J. Geophys. Res. Oceans, 121, 311–326.*
- *Cheriton, O., Storlazzi, C., Rosenberger, K. (2016) "Observations of wave transformation over a fringing coral reef and the importance of low-frequency waves and offshore water levels to runup, overwash, and coastal flooding." J. Geophys. Res. Oceans, v. 121, p. 1-20.*

I think the paper would benefit from a review of these studies either here or in other parts of the manuscript. Where possible, I also suggest the present results be compared (ideally quantitatively) with the results in these studies (and others cited in the manuscript), especially with previous lab results.

Response:

These studies are reviewed in the revised manuscript. Comparisons with previous studies are added now.

Line 73-76:

Similarly, may also refer to Nakaza and Hino (1991) and Nakaza et al (1991) on this subject.

- *Nakaza, E. and Hino, M. (1991), "Bore-like surf beat in a reef zone caused by wave groups of incident short period waves", Fluid Dynamics Research, 7, 89-100.*
- *Nakaza, E., Tsukayama, S., and Hino, M., (1991), "Bore-like surf beat on reef coasts", Proc., 22nd Int. Conf. Coastal Eng., ASCE, Reston, Va., 743–756.*

Response:

References are added.

Line 83:

The word "assess" (instead of figure out) can be a more appropriate choice.

Also, the last two sentences of this paragraph (lines 83-86) needs rewording and attention to grammar (e.g. an engineering solution, etc.)

Response:

Revised.

Line 89:

Consider the word "considered" (instead of conducted). Also please review the grammar: e.g. a platform reef, a fringing reef, etc.

Response:

Revised.

Line 92:

"after the introduction" is redundant. The introduction section is already presented.

Response:

Revised.

Line 94:

Section(s) 4 and 5.

Also "with a set of conclusions in …" probably best to be reworded. Could be written as ", followed by conclusions in section 6."

Response:

Revised.

Line 104-105:

Is it really necessary to state manufacturing country of the instruments?

Response:

Manufacturing country of the instrument is deleted.

Figure 1 and Line 106:

- *G1-15 and V1-4 needs to be defined/identified (as location of wave gauges and velocity meters) either as annotation on the Figure or in the text (Line #106) where the figure is first referred to.*
- *Caption of Figure 1 (below) unnecessarily repeats the same information twice; and needs to be revised: "Fig. 1. Measuring instrument arrangement and the reef model. (a) Measuring instrument arrangement; (b) Reef model."*

Response:

This is revised.

Line 108:

JONSWAP spectrum (all uppercase)

Response:

This is revised.

Line 133-134

"propagating to the landward" ----> propagating landwards

"propagating to the seaward" ----> propagating seawards

Response:

This is revised.

Line 136-144:

The two sentences in lines #137-139 are effectively a repeat of the opening sentence. The only new information they provide for the reader is about the location (Offshore and G7) associated with each sub-figure. This is simply redundant.

Current text:

"The incident wave envelope η_{env}*, filtered wave surface elevations of IG component* η_{IG} *and SS component* η_{SS} *are shown in Fig. 2. Fig. 2(a) depicts the water surface elevation of the incident wave and the incident wave envelope* η_{env} *calculated by Eq.*

(1). Fig. 2(b) shows the filtered wave surface elevations of IG componenet η_{IG} *and SS component* η_{SS} *at reef edge (G7). When the incident wave approaches the reef flat, the rapid decrease of the water depth leads to the strong wave deformation and violent wave breaking and the IG wave is then observed on the reef flat (G7-G15) …"*

Can be replaced, for instance, with:

"The incident wave envelope η_{env}*, filtered wave surface elevations of IG component* η_{IG} *and SS component* η_{SS} *are shown in Fig. 2. When incident waves (Fig. 2a) approach the reef edge (Fig. 2b), the rapid decrease in water depth leads to strong wave deformation and violent wave breaking, and the IG wave is then observed on the reef flat (G7-G15) …"*

Response:

This is simplified in the revised manuscript.

Line 146:

"As shown in Fig 3"

Figure 3 was just referred to in the previous line. It's just redundant to repeat the same thing in the next line.

Response:

Revised.

Line 151:

"In Schaffer (1993) …" is not a proper form of in-text citation.

Please reword to an appropriate style, e.g. "Schaffer (1993) showed/found that", etc.

Response:

Revised.

Line 153:

"Fig. 4 is the relationship …"

A figure can't be a relationship. Please reword. Figure 4 shows xyz, etc.

Response:

Revised.

Figure 4 (discussed in Lines 154-157)

Is this chart correct? I think fringing reef (red circles) should sit above the platform reef (black circles). Comparing this with data on other figures, I believe it's probably an incorrect chart legend. Please investigate or otherwise explain.

Response:

The chart legend in Fig. 4 is incorrect. This is Revised.

Line 156:

" ... is a little greater ..."

Please reword. e.g. "... is slightly larger..."

Response:

Revised.

Line 207-208

" ... For the fringing reef, the SS wave height has a small increase."

Please discuss the reason. Larger wave setup (in the case of a fringing reef), which subsequently provides a larger total water depth (hr + setup), is responsible for allowing larger (near-)equilibrium SS wave height near the shoreline.

Response:

The SS wave height on the reef flat is controlled by the water depth. For the fringing reef, the larger submergence depth $(\bar{\eta}_r + h_r)$ is responsible for the larger SS wave height.

This is discussed in section 4.

Line 213-214 (Figure 8a)

It appears from Figure 8a that Hss/(eta+hr) ratio is roughly 0.6. How does that compare with other studies and field/lab data? Hardy and Young (1996) data for instance seem to suggest 0.4. Baldock et al (2020) have 0.35.

- *Hardy, T. and Young, I. (1996) "Field study of wave attenuation on an offshore coral reef", J. Geophys. Res.: Oceans 101, 14311–14326.*

Response:

In the experiment, for the platform reef, the ratio γ of the SS wave height H_{ss} and submergence depth $(\bar{\eta}_r + h_r)$ in the inner surf zone ranges from 0.50 to 0.67. For the

fringing reef, the wave reflection and slamming on the vertical shoreline generate larger γ ranged from 0.56 to 0.75. This is added in the manuscript.

The wave height to water depth ratio γ over the reef flat observed in field observation was reviewed by Harris et al. (2018). The most common vale of γ observed on reef flats is between 0.4 to 0.6. The wave energy dissipation induced by the wave breaking and bed friction will lead to a small γ value in the inner reef flat. For example, field studies at John Brewer Reef in the central GBR indicate that the maximum significant wave height in the inner reef flat is 0.35-0.4 times the water depth over the reef flat (Hardy and Young, 1996). On One Tree Reef, γ value at the outer reef flat larger than 0.85 and decreases in the inner reef flat to 0.1 in the most pronounced case (Harris et al., 2018).

In our experiment, the vertical shoreline and smooth surface generate larger wave heights than the field observations.

Line 233:

"Fig. 8 shows the photos of the wave breaking around the reef edge at the same moment for the platform reef and fringing reef."

Should be Fig 9 instead of Fig 8.

Response:

Revised.

Experimental investigation on the infragravity wave on different reef systems under irregular wave action

Gancheng Zhu[1], Bing Ren[2*], Ping Dong[3], Guoyu Wang[4], Weidong Chen[5]

[1]Ph.D. candidate, State Key Laboratory of Coastal and Offshore Engineering, Dalian Univ. of Technology, Dalian 116024, China. Email: i191376645@mail.dlut.edu.cn

[2*]Professor, State Key Laboratory of Coastal and Offshore Engineering, Dalian Univ. of Technology, Dalian 116024, China (corresponding author). Email: bren@dlut.edu.cn

[3]Professor, School of Engineering, University of Liverpool, Liverpool, United Kingdom. Email: Ping.Dong@liverpool.ac.uk

[4]Associate Professor, State Key Laboratory of Coastal and Offshore Engineering, Dalian Univ. of Technology, Dalian 116024, China. Email: wanggyu@dlut.edu.cn

[5]Ph.D. candidate, State Key Laboratory of Coastal and Offshore Engineering, Dalian Univ. of Technology, Dalian 116024, China. Email: chenweidong1996@mail.dlut.edu.cn

Abstract

This paper presents the results of a laboratory investigation into the role of infragravity motions in reef hydrodynamics over different reef systems. Laboratory experiments are performed with reef profiles of a platform reef and a fringing reef under irregular wave conditions. The propagation and the distribution of the infragravity wave are different over these two reef systems. Analysis of the measured time histories of water surface elevation shows that shorter sea-swell (SS) waves, longer infragravity (IG) wave and mean water level on the reef flat are significantly larger in the fringing reef system. The IG wave height can be up to three times larger on the fringing reef than that on the platform reef. This marked increase of the IG wave is considered to be due to: (1) the superposition of incoming IG wave and reflected IG wave from shoreline; (2) more violent wave breaking in the surf zone that may enhance the transfer of wave energy from the frequency band of the shorter wave to IG wave. In this experiment, the wave breaking mechanism controls the relationship between IG wave height and water depth.

Keywords: Infragravity wave; Fringing reef; Platform reef; Shoreline; Wave set-up

1. Introduction

Million people worldwide live in coastal areas near coral reefs many of which form natural barriers protecting shorelines against waves, storms, and floods. Reef-lined coasts, however, are becoming increasingly vulnerable to wave-driven flooding as a result of climate change and the reef degradation caused by coastal developments for residents and the growing tourism industry. It is essential to understand the dynamic processes of the reef system either in the natural or built states.

Hydrodynamic interaction of waves with coral reefs is complex and has been studied over decades. The wave energy propagation on reefs can be very different from normal coastal beaches primarily because of the complex coastal configurations at various scales and the roughness of the substrate. A typical platform reef is often idealized to consist of a seaward sloping reef face and a shallow reef flat. For the fringing reef, the inshore reef flat extends toward the shoreline. The reef flat in shallow water is commonly exposed at low tide (Cabioch et al., 2010). Wave breaking induced by the shallow water significantly reduces most of the sea-swell wave energy ($f > 0.04$ Hz) (Gourlay, 1994) and the rough surface of the reef also causes a further dissipation of wave energy (Lowe et al., 2005; Buckley et al., 2016; Baldock et al., 2020). In field observations, coral reefs can provide defense against huge wave attack by reducing overall wave energy up to an average of 97% (Ferrario et al., 2014). However, infragravity wave (0.004~0.04 Hz) and wave set-up are found to be enhanced on the reef flat relative to mild coastlines (Becker et al., 2014; Becker et al., 2016; Bukley et al., 2018). As a consequence, infragravity wave (IG wave) is seen to play a significant role on the reef flat and in the lagoon (Péquignet et al., 2009; Pomeroy et al., 2012b; Van Dongeren et al., 2013) with IG wave becoming a dominant component to the wave run-up on the reef-fringed shoreline (Buckley et al.,2018).

Wave set-up which is the rise of the mean water level induced by the depth-limited wave breaking has been widely studied by field observations on coral-line coasts (Munk and Sargent, 1948; Vetter et al., 2010; Becker

et al., 2014), laboratory experiments (Gerritsen, 1980; Gourlay, 1996a; Yao et al., 2018) and theoretical analysis (Tait, 1972; Gourlay, 1996b; Yao et al., 2017; Zhu et al., 2019). The wave set-up on natural reefs is influenced by the incident wave height, water depth on the reef flat and the roughness of the reef (Franklin, 2013; Buckley et al., 2016). Wave set-up on the reef flat increases with the increase of the incident wave height and the decrease of the water depth on the reef flat (Gourlay, 1996a; Becker et al., 2014). The roughness of the reef has two opposite effects on the wave set-up: the frictional dissipation of wave energy seaward of the breakpoint results in a decrease of the wave set-up; the onshore-directed bottom stress induced by the offshore-directed near bottom velocity may lead to the increase of the wave set-up (Franklin et al., 2013; Bukley et al., 2016).

IG wave recognized as the low frequency (0.004~0.04 Hz) set-up/down oscillation is generated by two widely accepted mechanisms. The first mechanism is the release of the bound IG waves. The radiation stress gradient generates the bound IG wave in the incident wave groups (Longuet-Higgins and Stewart, 1962). When the water depth decreases and waves break, the bound IG waves are released and propagate as free waves. In the other mechanism, the IG waves are generated as dynamic set-up/down oscillations as a result of the spatially fluctuating breakpoints of different sized wave groups (Symonds et al., 1982). Along with the generation of the IG waves, the groupiness of the incident wave decreases due to the wave breaking (Liu and Li, 2018; Poate et al., 2020). Bound wave release is considered to be a more important source of IG wave on the gentle slope (List, 1992; Janssen et al., 2003). While for the steep slope, the time-varying breakpoint mechanism is considered to be the dominant mechanism for the generation of the IG wave (Battjes et al., 2004; Baldock et al., 2012). Many reefs have very steep slopes with some reef faces even being close to vertical (Gourlay, 1996b). Therefore in many field observations (Pomeroy et al., 2012a; Becker et al., 2016) and experiments (Buckley et al., 2018), IG waves on the reef flat are linked to the time variation of the wave breakpoint. In the surf zone, the wave breakpoint mechanism is also found working against the incident bound IG wave (Pequignet el al., 2014).

Although the IG wave on the reef flat is also damped by the roughness of the reef, the bottom friction has a much greater effect on the short waves than the IG waves (Pomeroy et al., 2012a). The IG wave has a bore-like wave shape (Gawehn et al., 2016). Due to the high propagation speed, the huge inertial forces at the front of the IG wave can cause extensive damage to coastal structures. For example, in the Okinawa islands of southern Japan, seawall, roads and houses sheltered by reef were found damaged by bore-like floods with 10-minutes intervals (Nakaza et al., 1991). During Typhoon Haiyan in 2013, video footage captured serious destruction to a Philippine town by fast-moving bore (Roeber and Bricker., 2015). When the frequencies of the IG wave are close to the natural frequencies of the water body on the reef flat, resonant amplification is possible and the coastal flooding potential increases (Cheriton et al., 2016; Gawehn et al., 2016). The IG wave can also lead to moored ship motions (Van Dongeren et al., 2016) and large resonance (Gao et al., 2019) for the reef-fringed harbors.

Besides the wave breaking, the infragravity wave is also influenced by the reef-fringed shoreline. On the platform reef, wave and current can escape to the sea through the end of the reef flat or lagoon. However, on the fringing reef, infragravity wave will be reflected by the shoreline and then propagate to the open sea or trapped on the reef flat. In order to assess the influence of the shoreline, comparison on the reef hydrodynamics between fringing reef and platform reef is needed. Based on which, an engineering solution that meets specific engineering, ecological criteria may be developed to ameliorate the coastal erosion and flooding.

This paper presents a two-dimensional laboratory experiment to investigate the hydrodynamic processes on an idealized reef under irregular wave conditions. Two different reef profiles are considered: a platform reef and a fringing reef. The generation and propagation of the IG wave on the reef flat are analyzed based on measurements of water surface elevation and flow velocity at 15 locations along the wave flume and the changes in the wave conditions on the reef flat caused by the shoreline are discussed. The paper is organized as below:

93 the experiment setup is introduced in section 2; the wave propagation and the generation of the IG wave are
94 presented in section 3; the influences of reef-fringed shoreline are discussed in sections 4 and 5 followed by
95 conclusions in section 6.

96 2. Experiment setup

97 Laboratory experiments were carried out in the State Key Laboratory of Coastal and Offshore Engineering,
98 Dalian University of Technology, Dalian. The flume is 60 m long, 4 m wide and 2.5 m depth. Zhu et al. (2018)
99 detailed the set of wave flume and the scaled physical models of the reef in regular wave tests. Here these
100 physical models were further used under the irregular wave conditions. The reef model consisted of a steep reef-
101 face with a slope of 1:1 and a horizontal reef flat of 8.6 m long. The reef face and reef flat were built by smooth
102 sand-cement grout, a relatively smooth and impervious surface. The process of wave run-up on the shoreline is
103 not taken into account, therefore the reef-fringed shoreline is adopted as a vertical structure which is 7.2 m away
104 from the reef-edge. Without the shoreline, the reef model is corresponding to a platform reef. Fig. 1 shows the
105 sketch of reef profile and measuring instrument arrangement. Fifteen capacitance wave gauges (TWG-600) and
106 four high resolution acoustic velocity meters (Vectrino) were installed to measure the wave surface elevation
107 and velocity. Locations of wave gauges (G1-G15) and velocity meters (V1-V4) are shown in Fig. 1. The
108 measuring accuracy of the wave gauge is ±0.1 mm. The measuring accuracy of the velocity meter is ±0.5% of
109 the measured value. The sampling rate of 50 Hz was used for all wave gauges and velocity meters.

110 Incident irregular waves were generated using the JONWSAP spectrum. The model test scale is taken as
111 1:25. The submergence water depths on the reef flat h_r and incident wave conditions tested in the experiments
112 are listed in Table 1. In total 24 different wave conditions were tested in the experiment. Each test was repeated
113 at least 3 times.

3. Generation and propagation of IG wave

The frequency of infragravity wave is commonly taken as from 0.004Hz to 0.04Hz. In the experiment, the model test scale is 1:25, so the corresponding frequency range of IG wave is 0.02-0.2 Hz. The wave surface elevation measured by the wave gauge is η. The average wave set-up $\bar{\eta}$ the rise of water level averaged on the whole acquisition time. The IG component η_{IG} and SS component η_{SS} were filtered based on their frequency ranges.

The wave envelope η_{env} of the incident wave group was calculated based on the Hilbert transform (Janssen et al., 2003):

$$\eta_{\mathrm{env}} = \left|\eta_{\mathrm{SS}} + i\Gamma(\eta_{\mathrm{SS}})\right| \tag{1}$$

where $\Gamma(...)$ denotes the Hilbert transform operator $\Gamma\big(f(t)\big) = \int f(t)\mathrm{e}^{-iwt}\mathrm{d}t$. The characteristic spectral wave heights of the IG wave and SS wave were calculated as

$$H_{\mathrm{IG}} = 4\sqrt{\int_{0.02}^{0.2} S_f df} \tag{2}$$

$$H_{\mathrm{SS}} = 4\sqrt{\int_{0.2} S_f df} \tag{3}$$

where S_f is the wave spectral density computed from the wave surface elevation with a segment length of 16384 samples. The characteristic spectral wave height of the incident wave was calculated by the spectral density $S_{f,\mathrm{in}}$ of the incident irregular wave:

$$H_{\mathrm{in}} = 4\sqrt{\int S_{f,\mathrm{in}} df} \tag{4}$$

The characteristic wave heights and the wave set-up $\bar{\eta}$ used the average values of repeated tests. The deviation from the average is calculated by the relative standard deviations (RSD):

$$\mathrm{RSD} = \sqrt{\frac{\sum_{i=1}^{n}(x_{\mathrm{i}} - \bar{x})^2}{n-1}} / \bar{x} \tag{5}$$

where $\bar{x}$ is the average value. The relative standard deviations of the characteristic wave height and the wave set-up at G15 are shown in Table 2. The small values of RSD indicate good test repeatability under different

136 wave conditions.

137 In this experiment, the incoming wave (propagating landwards) and outgoing wave (propagating seawards)
138 are separated based on the signals measured from the wave gauges and the velocity meters at the same position
139 (V1-V4 in Fig. 1) in a way similar to that of Buckley et al.'s (2015).

140 The incident wave envelope η_{env}, filtered wave surface elevations of IG component η_{IG} and SS
141 component η_{SS} are shown in Fig. 2. When the incident wave (Fig. 2a) approaches the reef edge (Fig. 2b), the
142 rapid decrease of the water depth leads to the strong wave deformation and violent wave breaking, then the IG
143 wave is observed on the reef flat (G7-G15). The wave surfaces of SS wave and IG wave have bore-like shapes.
144 As shown in Fig. 2(b), the wave surface of IG wave on the reef flat is in phase with the SS wave group, which
145 is evidence that the IG wave is generated by the time-varying breaking point mechanism (Symonds et al., 1982;
146 Pomeroy et al., 2012a).

147 Wave spectral densities S_f of different wave gauges are shown in Fig. 3 with the dotted line indicating
148 the spectral densities of incident wave envelope η_{env}. The SS wave is dominant in the incident wave. As waves
149 break on the reef edge at G7, the SS wave energy decreases significantly due to the wave breaking and the IG
150 wave is generated. The frequency of the IG wave mainly depends on the incident wave envelope as the time-
151 varying breakpoint mechanism is dominant in this experiment. Out of the surf zone (G15), the IG wave is
152 dominant, especially for the fringing reef.

153 Schäffer (1993) found that the IG wave height has a positive correlation with the wave height variation of
154 the incident wave group. For the irregular wave, the wave height variation of the wave group can be revealed
155 by the standard deviations σ_{env} of η_{env}. Fig. 4 shows the relationship between σ_{env} and the IG wave height
156 H_{IG} on the reef flat at G15. A strong linear correlation is clearly observed between σ_{env} and the IG wave
157 height H_{IG}. Due to that the increase of the wave period may lead to an increase in the wave groupiness

158 (Karunarathna et al., 2005), σ_{env} for significant period $T_{\mathrm{s}} = 2.0$ s, is a slightly larger than that for $T_{\mathrm{s}} = 1.5$ s.

159 Therefore, the IG wave height H_{IG} on the reef flat is larger in general when $T_{\mathrm{s}} = 2.0$ s.

160 Based on the incident wave envelope η_{env} and the IG wave surface η_{IG} at different measuring points,

161 the cross correlation $R_{\mathrm{eI}}(\tau)$ can be calculated (Janssen et al., 2003) as

162 $$R_{\mathrm{eI}}(\tau) = \frac{\langle \eta_{\mathrm{env}}(t)\eta_{\mathrm{IG}}(t+\tau) \rangle}{\sigma_{\mathrm{env}}\sigma_{\mathrm{IG}}} \tag{6}$$

163 where $\langle ... \rangle$ is the time averaging operator, τ is the time lag between η_{env} and η_{IG}, σ_{env} and σ_{IG} are

164 standard deviations of η_{env} and η_{IG} respectively. Fig. 5 shows the cross correlation $R_{\mathrm{eI}}(\tau)$ between the

165 incident wave envelope η_{env} and the IG wave surface η_{IG} at different measuring points. The generation and

166 propagation of the IG waves are revealed by the color map of $R_{\mathrm{eI}}(\tau)$ under different time lags τ. The dotted

167 lines in Fig. 5(b) are the theoretical path of the IG waves. Based on the theoretical speed of the incident wave

168 group, the theoretical path of bound IG wave in the incident wave group is shown as Path 1. Paths 2-6 are the

169 theoretical path of free IG wave, which is calculated by the wave velocity related to the local water depth. Due

170 to that the bound IG wave in the incident wave group is small, no obvious negative correlation is found along

171 Path 1.

172 When waves propagate onto the reef flat, the breaking of the incident wave group generates IG waves.

173 Therefore on the reef flat (x >1.8 m), clear positive correlation is observed (Path 3). The wave breaking of the

174 wave group can also generate outgoing IG waves, as shown along Path 2 (negative correlation). Previous

175 researches on the time-varying breakpoint mechanism showed that the incoming IG wave is in phase with the

176 wave group and the outgoing IG wave has a phase difference of 180° with the wave group (Baldock et al., 2012;

177 Contardo and Symonds, 2013). The same is found in the results of this experiment, confirming that in this

178 experiment both the incoming and outgoing IG waves are generated by the time-varying breakpoint mechanism.

179 For the fringing reef, the incoming IG wave reflects from shoreline (Path 4). However, the reflected outgoing

IG waves do not propagate further out to the open sea as Path 6 shows. The possible reason is that the rapid change of the water depth around the reef edge leads to a wave reflection as Path 5 shows. It is worthy noticing that the cross correlation along Path 5 is relatively small.

4. Distributions of wave height and wave set-up on the reef flat

Wave set-up $\bar{\eta}$, IG wave height H_{IG} and SS wave height H_{SS} are nondimensionalized by the wave height of the incident wave height H_{in}. The distributions of $\bar{\eta}/H_{\mathrm{in}}$, $H_{\mathrm{IG}}/H_{\mathrm{in}}$ and $H_{\mathrm{SS}}/H_{\mathrm{in}}$ are shown in Fig. 6. As expected, IG wave height and wave set-up increases in the surf zone. For the platform reef, when the water depth on the reef flat is small ($h_{\mathrm{r}} < 5$ cm), the large values of IG wave height and wave set-up are found at the reef edge (G7). The maximum of the IG wave height may occur at the reef edge as shown in Fig. 6 (d-e). Then the IG wave height decreases rapidly at G8 and increases gradually along the reef flat.

For the platform reef, the wave propagation over the reef edge under different water depths is shown in Fig. 7. When the water depth is small, the wave overtopping on the reef edge generates an obvious increase of the water level. It leads to the large wave set-up and IG wave at G7. As shown in Fig.7(a-c), the high water level at reef edge accelerates the flow propagating landwards and the water level decreases quickly around G8. For the platform reef, the time series of wave surface elevation η and IG wave component η_{IG} at G7 and G8 are shown in Fig. 8. The time series also show a decrease of water level from G7 to G8. Therefore, the wave set-up and IG wave have a rapid decrease around the reef edge. In our experiment, the outer reef flat (G8-G13) is the surf zone. The wave breaking in the surf zone brings the increase of wave set-up and IG wave height (G8-G13). Then the wave set-up and IG wave height tend to be stable (G13-G15). When the water depth increases, there is no obvious wave overtopping over the reef edge, as shown in Fig. 7(d-f). Therefore, the wave set-up and IG wave height increase along the reef flat due to the wave breaking.

For the fringing reef, the reef flat is blocked by the shoreline. Wave overtopping over the reef edge can not generate flow propagating shoreward. Therefore, the rapid decreases of wave set-up and IG wave height cease to occur at the reef edge. The suppression of the wave-induced flow leads to a further rise of the mean water level, as shown in Fig. 6(a-c). The scatters in Fig. 6(d-f) are the separated incoming and outgoing IG wave heights. The vertical shoreline in this experiment leads to a complete reflection of the incoming IG wave. The IG wave is larger than that for the platform reef. For example, as shown in Fig. 6(d-f), the relative IG wave height $H_{\mathrm{IG}}/H_{\mathrm{in}}$ is about 0.2 on the platform reef. For the fringing reef, the relative IG wave height $H_{\mathrm{IG}}/H_{\mathrm{in}}$ in front of the shoreline is about 0.6, increases by a factor of 3. The scatters in Fig. 6(d-f) are the separated IG wave heights of the incoming and outgoing IG waves. It can be seen that the vertical shoreline in this experiment leads to a complete reflection of the incoming IG wave.

As shown in Fig. 6(g-i), the SS wave height decreases rapidly in the surf zone. Outside the surf zone, the SS wave height is almost constant as a result of the smooth reef surface in the experiment. For the fringing reef, the submergence depth $(\bar{\eta}_{\mathrm{r}} + h_{\mathrm{r}})$ increases, which leads to a small increase of the SS wave height.

5. Wave heights in front of the shoreline

The wave heights in front of the shoreline are shown in Fig. 9. The horizontal axis is the non-dimensional submergence depth on the reef flat ($(\bar{\eta}_{\mathrm{r}} + h_{\mathrm{r}})/H_{\mathrm{in}}$), where $\bar{\eta}_{\mathrm{r}}$ is the wave set-up at G15. Fig. 9(a) shows the relative SS wave height $H_{\mathrm{SS}}/H_{\mathrm{in}}$ in front of the shoreline (G15). It can be seen that the SS wave height is proportional to the water depth, as a result of the SS wave heights being limited by the submergence depth on the reef flat. For the platform reef, the ratio γ of the SS wave height H_{ss} and submergence depth $(\bar{\eta}_{\mathrm{r}} + h_{\mathrm{r}})$ in the inner surf zone ranges from 0.50 to 0.67. For the fringing reef, the wave reflection and slamming on the

222 vertical shoreline generate larger γ ranged from 0.56 to 0.75.

223 Fig. 9(b) shows the relative IG wave height $H_{\mathrm{IG}}/H_{\mathrm{in}}$ in front of the shoreline at G15. For the fringing reef,
224 the IG wave height has significant increase by a factor of 2-3. Therefore, the IG wave heights in front of the
225 shoreline remain quite high as the relative IG wave height is from 0.49-0.68 under different wave conditions.
226 The obvious reason for the significant increase of the IG wave height is the perfect wave reflection from the
227 shoreline. With a gentle shoreline, the IG wave height will decrease due to the decrease of the wave reflection.
228 For the fringing reef, the wave heights of the separated incoming IG wave at G15 are shown in Fig. 9(b). It can
229 be seen that the incoming IG wave heights are also larger than the IG wave heights for the platform reef. Fig.
230 9(c) shows the relative IG wave heights $H_{\mathrm{IG}}/H_{\mathrm{in}}$ at G6. The IG waves at G6 are considered as the outgoing IG
231 waves generated in the surf zone (Path 2 in Fig. 5). For the fringing reef, the outgoing IG wave heights at G6
232 also increase as shown in Fig. 9(c). These phenomena indicate that with the shoreline, the wave breaking in the
233 surf zone may generate larger outgoing (Path 2) and incoming (Path 1) IG waves. Fig. 10 shows the photos of
234 the wave breaking around the reef edge at the same moment for the platform reef and fringing reef. It can be
235 seen that with the shoreline, the wave generated flow can't flow out of the reef flat and the high water level on
236 the reef flat generates strong backflow (Zhu et al., 2018) which in turn induces a more violent wave breaking.
237 As a consequence, for the fringing reef, the outgoing (Path 2) and incoming (Path 1) IG waves generated in the
238 surf zone may increase.

239 The ratio of the IG wave height and SS wave height $H_{\mathrm{IG}}/H_{\mathrm{SS}}$ at G15 are shown in Fig. 9(d). When
240 submergence depth decreases, IG wave plays a more important role on the reef flat. For the fringing reef, the
241 values of $H_{\mathrm{IG}}/H_{\mathrm{SS}}$ are more than 1 in general, which indicates IG wave dominance under all submergence
242 depth. In the case of the real reef, the bottom friction has a much greater effect on damping the short waves
243 compared to the IG waves (Pomeroy et al., 2012a) and the SS wave in front of the shoreline may become even

smaller.

For the fringing reef, Comparisons of IG wave height between our experiment and previous studies are shown in Table A1. Due to the steep reef face, the vertical shoreline and smooth surface, our experiment have the largest relative IG wave heights (0.49-0.68). The field observations have smaller IG wave height on the reef flat than the laboratory experiments with smooth surface.

In field observations (Pomeroy et al., 2012a; Gawehn et al., 2016), the IG wave was found to increase notably with the increase of the submergence depth. They attribute this to the bottom friction or reef resonance. When the water depth increases, the wave energy dissipation induced by the bottom friction decreases (Pomeroy et al., 2012a). Larger water depth on the reef flat also increases the probability of resonance (Gawehn et al., 2016). When water depth increases, the resonance and the decrease of the wave energy dissipation lead to a large IG wave heights on the reef flat. However, when the bottom friction is small, this proportional relationship will disappear. For example, in Beetham et al.'s (2015) field observation, the IG wave height is minimally affected by the water depth. Nwogu and Demirbilek's (2010) and Yao et al.'s (2020) laboratory experiment results are reanalyzed in dimensionless forms, as shown in Fig. 11. Different from field observations, the IG wave height decreases with the increase of the submergence depth in our experiment and Yao et al.'s (2020) experiment. The efficiency of the breakpoint mechanism decreasing as the water depth over the reef increases, which results in a decrease generation of IG wave in the surf zone. When the bottom friction is small enough to be neglected, the wave breaking mechanism will control an opposite relationship between IG wave height and water depth. Noticeably, Nwogu and Demirbilek's (2010) experiments show a different trend due to the obvious reef resonance at large water depth. Therefore, when water depth increases, the IG wave height is influenced by these three factors which act counter to each other. However, the efficiency of the breakpoint mechanism seems to be a less important factor than bottom friction and resonance.

6. Conclusions

In order to investigate the hydrodynamic processes on an idealized reef under irregular wave conditions, a two-dimensional experiment is carried out. Strong IG waves are generated on the reef flat by the time-varying breakpoint mechanism. The IG wave height on the reef flat is proportional to the standard deviations σ_{env} of the incident wave envelope η_{env}. The larger significant period T_{s} of the incident wave leads to a larger IG wave height on the reef flat.

Different with the field observations, the IG wave height is found to decrease slightly with the increase of the submergence depth. The efficiency of the breakpoint mechanism decreasing as the water depth over the reef increases, which results in a reduction of IG wave generated inside the surf zone. In the case of the real reef, bottom stress, reef resonance and wave breaking all have influence on the IG wave height. However, the efficiency of the breakpoint mechanism seems to be a less important factor.

For the fringing reef, the wave set-up, SS wave height and IG wave height on the reef flat all show varying degrees of increase. IG wave height can be even three times larger in the presence of the vertical shoreline. Two reasons are responsible for this increase of the IG wave: (1) the superposition of incoming IG wave and reflected IG wave and (2) more violent wave breaking in the surf zone. Because that the SS wave height is more strongly limited by the shallow water depth on the reef flat, the SS wave in front of the shoreline plays a much less important role than the IG wave does. The IG wave should be considered as the most important factor especially in the fringing reef system. The relative large size of the IG wave heights on the fringing reef and on the platform reef is observed under the specific setup of the experiment such as a vertical wall, smooth surface and steep reef face. Must more tests will also be required to assess fully the effects of the distance and front slope on IG wave propagation to develop a more general relationship between the relative wave height and these controlling parameters.

CRediT authorship contribution statement

Gancheng Zhu: Investigation, Methodology, Writing - original draft, Formal analysis. **Bing Ren**: Validation, Methodology, Funding acquisition, Supervision, Writing - review & editing. **Dong Ping**: Supervision, Writing - review & editing, Formal analysis. **Guoyu Wang**: Writing - review & editing, Formal analysis. **Weidong Chen**: Formal analysis.

Declaration of competing interest

The authors declare that they have no known competing financial interests or personal relationships that could have appeared to influence the work reported in this paper.

Acknowledgments

This work was supported by the National Natural Science Foundation of China under Grant No. 51979028.

Appendix A

Field observations and laboratory experiments are compared with our experiment results in Table A1. The IG wave heights mearsued in thes studies are transformed to the characteristic wave height H_{IG}.

References

Baldock, T.E., 2012. Dissipation of incident forced long waves in the surf zone-Implications for the concept of ‘‘bound’’ wave release at short wave breaking. Coast. Eng. 60, 276–285. https://doi.org/10.1016/j.coastaleng.2011.11.002.

Baldock, T.E., Shabani, B., Callaghan, D.P., Hu, Z., Mumby, P.J., 2020. Two-dimensional modelling of wave dynamics and wave forces on fringing coral reefs. Coast. Eng. 155, 103594.

https://doi.org/10.1016/j.coastaleng.2019.103594.

Battjes, J.A., Bakkenes, H.J., Janssen, T.T., van Dongeren, A.R., 2004. Shoaling of sub- harmonic gravity waves. J. Geophys. Res. 109(C2). http://dx.doi.org/10.1029/ 2003JC001863.

Becker, J.M., Merrifield, M.A., Ford, M., 2014. Water level effects on breaking wave setup for Pacific Island fringing reefs. J. Geophys. Res.-Oceans 119, 914–932. https://doi.org/10.1002/2013JC009373.

Becker, J.M., Merrifield, M.A., Yoon, H., 2016. Infragravity waves on fringing reefs in the tropical Pacific: Dynamic setup. J. Geophys. Res.-Oceans 121, 3010–3028. https://doi.org/10.1002/2015JC011516.

Beetham, E., Kench, P., O'Callaghan, J., and Popinet, S., 2016, Wave transformation and shoreline water level on Funafuti Atoll, Tuvalu. J. Geophys. Res. Oceans 121, 311–326. https://doi.org/10.1002/2015JC011246.

Buckley, M.L., Lowe, R.J., Hansen, J.E., Van Dongeren, A.R., 2015. Dynamics of wave setup over a steeply sloping fringing reef. J. Phys. Oceanogr. 45 (12), 3005-3023. https://doi.org/10.1175/JPO-D-15-0067.1.

Buckley, M.L., Lowe, R.J., Hansen, J.E., Van Dongeren, A.R., 2016. Wave setup over a fringing reef with large bottom roughness. J. Phys. Oceanogr. 46 (8), 2317-2333. https://doi.org/10.1175/JPO-D-15-0148.1.

Buckley, M.L., Lowe, R.J., Hansen, J.E., Van Dongeren, A.R., Storlazzi, C.D., 2018. Mechanisms of wave-driven water level variability on reef-fringed coastlines. J. Geophys. Res.-Oceans 123 (5), 3811-3831. https://doi.org/10.1029/2018JC013933.

Cabioch, G., Davies, P., Done, T., Gischler, E., Macintyre, I. G., Wood, R. and Woodroffe, C., 2010. Encyclopedia of modern coral reefs: structure, form and process. Springer Science & Business Media.

Cheriton, O., Storlazzi, C., Rosenberger, K., 2016. Observations of wave transformation over a fringing coral reef and the importance of low-frequency waves and offshore water levels to runup, overwash, and coastal flooding. J. Geophys. Res. Oceans 121 (5), 3121-3140. https://doi.org//10.1002/2015JC011231.

Contardo, S., Symonds, G., 2013. Infragravity response to variable wave forcing in the nearshore. J. Geophys.

330 Res.-Oceans 118 (12), 7095-7106. https://doi.org/10.1002/2013JC009430.
331 Ferrario, F., Beck, M. W., Storlazzi, C. D., Micheli, F., Shepard, C.C, Airoldi, L., 2014. The effectiveness of
332 coral reefs for coastal hazard risk reduction and adaptation. Nat. Commun. 5, 3794.
333 https://doi.org/10.1038/ncomms4794.
334 Franklin, G., Mariño-Tapia, I., Torres-Freyermuth, A., 2013. Effects of reef roughness on wave setup and surf
335 zone currents. J. Coast. Res. 65 (sp2), 2005-2011. https://doi.org/10.2112/SI65-339.1.
336 Gao, J., Zhou, X., Zhou, L., Zang, J., Chen, H., 2019. Numerical investigation on effects of fringing reefs on
337 low-frequency oscillations within a harbor. Ocean Eng. 172, 86-95.
338 https://doi.org/10.1016/j.oceaneng.2018.11.048.
339 Gawehn, M., Van Dongeren, A., Van Rooijen, A., Storlazzi, C.D., Cheriton, O.M., Reniers, A., 2016.
340 Identification and classification of very low frequency waves on a coral reef flat. J. Geophys. Res.-Oceans
341 121 (10): 7560-7574. https://doi.org/10.1002/2016JC011834.
342 Gerritsen, F., 1980. Wave attenuation and wave set-up on a coastal reef. Coastal Engineering 1980, 444-461.
343 Gourlay, M.R., 1994. Wave transformation on a coral reef. Coast. Eng. 23(1-2), 17-42.
344 https://doi.org/10.1016/0378-3839(94)90013-2.
345 Gourlay, M.R., 1996a. Wave set-up on coral reefs. 1. Set-up and wave-generated flow on an idealised two
346 dimensional horizontal reef. Coast. Eng. 27, 161-193. https://doi.org/10.1016/0378-3839(96)00008-7.
347 Gourlay, M.R., 1996b. Wave set-up on coral reefs. 2. Set-up on reefs with various profiles. Coast. Eng. 28, 17-
348 53. https://doi.org/10.1016/0378-3839(96)00009-9.
349 Janssen, T.T., Battjes, J.A., Van Dongeren, A.R., 2003. Long waves induced by short-wave groups over a sloping
350 bottom. J. Geophys. Res.-Oceans. 108 (C8), 3252. https://doi.org/10.1029/2002JC001515.
351 Karunarathna, H., Chadwick, A., Lawrence, J., 2005. Numerical experiments of swash oscillations on steep and

352 gentle beaches. Coast. Eng. 52 (6), 497-511. https://doi.org/10.1016/j.coastaleng.2005.02.003.
353 Longuet-Higgins, M.S., Stewart, R.W., 1962. Radiation stress and mass transport in gravity waves, with
354 application to surf beats. J. Fluid Mech. 13, 481–504. https://doi.org/10.1017/S0022112062000877.
355 Lowe, R.J., Falter, J.L., Bandet, M.D., Pawlak, G., Atkinson, M.J., Monismith, S.G., Koseff, J.R., 2005. Spectral
356 wave dissipation over a barrier reef. J. Geophys. Res.-Oceans., 110(C4).
357 https://doi.org/10.1029/2004JC002711.
358 List, J.H., 1992. A model for the generation of 2-dimensional surf beat. J. Geophys. Res.-Oceans 97, 5623–
359 5635. https://doi.org/10.1029/91JC03147.
360 Liu, Y., Li, S., 2018. Variation of wave groupiness across a fringing reef. J. Waterw. Port Coast. Ocean Eng.,
361 144 (6), 04018022. https://10.1061/(ASCE)WW.1943-5460.0000475.
362 Munk, W.H., Sargent, M.C., 1948. Adjustment of Bikini Atoll to ocean waves. Trans. Am. Geophys. Union 29,
363 855–860. https://doi.org/10.1029/TR029i006p00855.
364 Nakaza, E., Tsukayama, S., Hino, M., 1991. Bore-like surf beat on reef coasts. Coastal Engineering 1990. 743-
365 756.
366 Nwogu, O., Demirbilek, Z., 2010. Infragravity wave motions and runup over shallow fringing reefs. Journal of
367 waterway, port, coastal, and ocean engineering. 136(6), 295-305.
368 https://doi.org/10.1061/(ASCE)WW.1943-5460.0000050.
369 Péquignet, A., Becker, J.M., Merrifield, M.A., Aucan, J., 2009. Forcing of resonant modes on a fringing reef
370 during tropical storm Man-Yi. Geophys. Res. Lett. 36, L03607. https://doi.org/10.1029/2008GL036259.
371 Pequignet, A., Becker, J., and Merrifield, M., 2014. Energy transfer between wind waves and low-frequency
372 oscillations on a fringing reef, Ipan, Guam. J. Geophys. Res. Oceans, 119, 6709–6724.
373 https://doi.org//10.1002/2014JC010179.

374 Poate, T., Masselink, G., Austin, M.J., Inch, K., Dickson, M., and McCall, R., 2020. Infragravity wave
375 generation on shore platforms: Bound long wave versus breakpoint forcing. Geomorphology, 350, 106880.
376 Pomeroy, A., Lowe, R.J., Symonds, G., Van Dongeren, A.R., and Moore, C., 2012a. The dynamics of
377 infragravity wave transformation over a fringing reef. J. Geophys. Res. 117, C11022. https://doi.org/
378 10.1029/2012JC008310.
379 Pomeroy, A., Van Dongeren, A., Lowe, R., van Thiel de Vries, J. and Rovelvink, J., 2012b. Low frequency wave
380 resonance in fringing reef environments. Coastal Eng. Proc. (33), 25-25.
381 https://doi.org/10.9753/icce.v33.currents.25.
382 Roeber, V., Bricker, J.D., 2015. Destructive tsunami-like wave generated by surf beat over a coral reef during
383 Typhoon Haiyan. Nat. Commun. 6, 7854. https://doi.org/10.1038/ncomms8854.
384 Schäffer, H.A., 1993. Infragravity waves induced by short-wave groups. J. Fluid Mech. 247, 551-588.
385 https://doi.org/10.1017/S0022112093000564.
386 Symonds, G., Huntley, D.A., and Bowen, A.J., 1982. Two-dimensional surf beat: Long wave generation by a
387 time-varying breakpoint. J. Geophys. Res. 87, 492–498. https://doi.org/10.1029/JC087iC01p00492.
388 Tait, R.J., 1972. Wave set-up on coral reefs. J. Geophys. Res. 77, 2207-2211.
389 https://doi.org/10.1029/JC077i012p02207.
390 Van Dongeren, A., Lowe, R., Pomeroy, A., Trang, D., Roelvink, J., Symonds, G., and Ranasinghe, R., 2013.
391 Numerical modeling of low-frequency wave dynamics over a fringing coral reef. Coast. Eng. 73, 178-190.
392 https://doi.org/10.1016/j.coastaleng.2012.11.004.
393 Van Dongeren, A., De Jong, M., Van der Lem, C., Van Deyzen, A., Den Bieman, J., 2016. Review of long wave
394 dynamics over reefs and into ports with implication for port operations. J. Mar. Sci. Eng. 4(1), 12.
395 https://doi.org/10.3390/jmse4010012.

Vetter, O., Becker, J.M., Merrifield, M.A., Pequignet, A.C., Aucan, J., Boc, S.J., Pollock, C.E., 2010. Wave setup over a Pacific Island fringing reef. J. Geophys. Res.-Oceans. 115 (C12). https://doi.org/10.1029/2010JC006455.

Yao, Y., He, W., Du, R., Jiang, C., 2017. Study on wave-induced setup over fringing reefs in the presence of a reef crest. Appl. Ocean Res. 66,164-177. http://doi.org/10.1016/j.apor.2017.06.002.

Yao, Y., Huang, Z., He, W., Monismith, S.G., 2018. Wave-induced setup and wave-driven current over Quasi-2DH reef-lagoon-channel systems. Coast. Eng. 138, 113-125. https://doi.org/10.1016/j.coastaleng.2018.04.009.

Zhu, G, Xia, Y, Ren, B, Wang, G., 2018. The influence of vertical-Wall structure on monochromatic wave propagation characteristics Over the deep-Sea Coral reefs. The 28th International Ocean and Polar Engineering Conference. International Society of Offshore and Polar Engineers.

Zhu, G., Ren, B., Wen, H., Wang, Y., Wang, C., 2019. Analytical and experimental study of wave setup over permeable coral reef. Appl. Ocean Res. 90, 101859. https://doi.org/10.1016/j.apor.2019.101859.

Figure captions

Fig. 1. Experiment set-up. (a) Measuring instrument arrangement; (b) Reef model.

Fig. 2. Wave surface elevations (h_r = 0.05 m, T_s = 2.0 s, H_s = 0.2 m). (a) Incident wave and wave envelope η_{env}; (b) Filtered wave surface at G7; (c) Filtered wave surface at G15.

Fig. 3. Wave spectral densities S_f (h_r = 0.05 m, T_S = 2.0 s, H_S = 0.2 m). (a) Platform reef; (b) Fringing reef.

Fig. 4. Relationship between σ_{env} and the IG wave height H_{IG} on the reef flat (G15).

Fig. 5. Cross correlation $R_{eI}(\tau)$ between the incident wave envelope η_{env} and the IG wave surface η_{IG} (h_r = 0.05 m, T_s = 2.0 s, H_s = 0.2 m). (a) Platform reef; (b) Fringing reef.

Fig. 6. Distributions of the relative wave set-up and relative wave height. (a-c) Wave set-up; (d-f) IG wave height. (g-i) SS wave height.

Fig. 7. Wave propagation over the reef edge for the platform reef (a-c) h_r = 0.00 m, T_s = 1.5 s, H_s = 0.2 m; (d-f) h_r = 0.10 m T_s = 1.5 s, H_s = 0.2 m.

Fig. 8. Wave surface elevations at G7 and G8 for platform reef (h_r = 0.00 m, T_s = 2.0 s, H_s = 0.2 m).

Fig. 9. Relationship between wave height and non-dimensional submergence depth on the reef flat. (a) Relative SS wave height H_{SS}/H_{in} at G15; (b) Relative IG wave height H_{IG}/H_{in} at G15; (c) Relative IG wave height H_{IG}/H_{in} at G6; (d) Ratio of IG wave height and SS wave height H_{IG}/H_{SS} at G15.

Fig. 10. Wave breaking around the reef edge. (a) Platform reef; (b) Fringing reef.

Fig. 11. Distribution of IG wave height for different larboratory experiments.

Table captions

Table 1 Water depth on the reef flat and incident wave conditions.

Table 2 Relative standard deviations at G15.

Table A1 Infragravity wave heights in field observations and laboratory experiments

Experimental investigation on the infragravity wave on different reef systems under irregular wave action

Gancheng Zhu[1], Bing Ren[2*], Ping Dong[3], Guoyu Wang[4], Weidong Chen[5]

[1]Ph.D. candidate, State Key Laboratory of Coastal and Offshore Engineering, Dalian Univ. of Technology, Dalian 116024, China. Email: i191376645@mail.dlut.edu.cn

[2*]Professor, State Key Laboratory of Coastal and Offshore Engineering, Dalian Univ. of Technology, Dalian 116024, China (corresponding author). Email: bren@dlut.edu.cn

[3]Professor, School of Engineering, University of Liverpool, Liverpool, United Kingdom. Email: Ping.Dong@liverpool.ac.uk

[4]Associate Professor, State Key Laboratory of Coastal and Offshore Engineering, Dalian Univ. of Technology, Dalian 116024, China. Email: wanggyu@dlut.edu.cn

[5]Ph.D. candidate, State Key Laboratory of Coastal and Offshore Engineering, Dalian Univ. of Technology, Dalian 116024, China. Email: chenweidong1996@mail.dlut.edu.cn

Abstract

This paper presents the results of a laboratory investigation into the role of infragravity motions in reef hydrodynamics over different reef systems. Laboratory experiments are performed with reef profiles of a platform reef and a fringing reef under irregular wave conditions. The propagation and the distribution of the infragravity wave are different over these two reef systems. Analysis of the measured time histories of water surface elevation shows that shorter sea-swell (SS) waves, longer infragravity (IG) wave and mean water level on the reef flat are significantly larger in the fringing reef system. The IG wave height can be up to three times larger on the fringing reef than that on the platform reef. This marked increase of the IG wave is considered to be due to: (1) the superposition of incoming IG wave and reflected IG wave from shoreline; (2) more violent wave breaking in the surf zone that may enhance the transfer of wave energy from the frequency band of the shorter wave to the IG wave. In this experiment, the wave breaking mechanism controls the relationship between IG wave height and water depth.

Keywords: Infragravity wave; Fringing reef; Platform reef; Shoreline; Wave set-up

1. Introduction

Million people worldwide live in coastal areas near coral reefs many of which form natural barriers protecting shorelines against waves, storms, and floods. Reef-lined coasts, however, are becoming increasingly vulnerable to wave-driven flooding as a result of climate change and the reef degradation caused by coastal developments for residents and the growing tourism industry. It is essential to understand the dynamic processes of the reef system either in the natural or built states.

Hydrodynamic interaction of waves with coral reefs is complex and has been studied over decades. The wave energy propagation on reefs can be very different from normal coastal beaches primarily because of the complex coastal configurations at various scales and the roughness of the substrate. A typical platform reef is often idealized to consist of a seaward sloping reef face and a shallow reef flat. For the fringing reef, the inshore reef flat extends toward the shoreline. The reef flat in shallow water is commonly exposed at low tide (Cabioch et al., 2010). Wave breaking induced by the shallow water significantly reduces most of the sea-swell wave energy (f >0.04 Hz) (Gourlay, 1994) and the rough surface of the reef also causes a further dissipation of wave energy (Lowe et al., 2005; Buckley et al., 2016; Baldock et al., 2020). In field observations, coral reefs can provide defense against huge wave attack by reducing overall wave energy up to an average of 97% (Ferrario et al., 2014). However, infragravity wave (0.004~0.04 Hz) and wave set-up are found to be enhanced on the reef flat relative to mild coastlines (Becker et al., 2014; Becker et al., 2016; Bukley et al., 2018). As a consequence, infragravity wave (IG wave) is seen to play a significant role on the reef flat and in the lagoon (Péquignet et al., 2009; Pomeroy et al., 2012b; Van Dongeren et al., 2013) with IG wave becoming a dominant component to the wave run-up on the reef-fringed shoreline (Buckley et al.,2018).

Wave set-up which is the rise of the mean water level induced by the depth-limited wave breaking has been widely studied by field observations on coral-line coasts (Munk and Sargent, 1948; Vetter et al., 2010; Becker

Commented [A1]: *Reviewer 2:*
Line 39-41:
Here, when discussing the propagation and dissipation of short-wave energy on reefs, I suggest citing some of the existing studies in that area. Baldock et al (2020) is a recent one on the subject. References therein are also useful.
•Baldock, E., Shabani, B., Callaghan, D., Zhifang, H., Mumby, P. (2020), "Two-dimensional modelling of wave dynamics and wave forces on fringing coral reefs", Coastal Engineering, 155, 103594.
Response:
Some of the existing studies are cited in the revised manuscript now.

et al., 2014), laboratory experiments (Gerritsen, 1980; Gourlay, 1996a; Yao et al., 2018) and theoretical analysis (Tait, 1972; Gourlay, 1996b; Yao et al., 2017; Zhu et al., 2019). The wave set-up on natural reefs is influenced by the incident wave height, water depth on the reef flat and the roughness of the reef (Franklin, 2013; Buckley et al., 2016). Wave set-up on the reef flat increases with the increase of the incident wave height and the decrease of the water depth on the reef flat (Gourlay, 1996a; Becker et al., 2014). The roughness of the reef has two opposite effects on the wave set-up: the frictional dissipation of wave energy seaward of the breakpoint results in a decrease of the wave set-up; the onshore-directed bottom stress induced by the offshore-directed near bottom velocity may lead to the increase of the wave set-up (Franklin et al., 2013; Bukley et al., 2016).

IG wave recognized as the low frequency (0.004~0.04 Hz) set-up/down oscillation is generated by two widely accepted mechanisms. The first mechanism is the release of the bound IG waves. The radiation stress gradient generates the bound IG wave in the incident wave groups (Longuet-Higgins and Stewart, 1962). When the water depth decreases and waves break, the bound IG waves are released and propagate as free waves. In the other mechanism, the IG waves are generated as dynamic set-up/down oscillations as a result of the spatially fluctuating breakpoints of different sized wave groups (Symonds et al., 1982). Along with the generation of the IG waves, the groupiness of the incident wave decreases due to the wave breaking (Liu and Li, 2018; Poate et al., 2020). Bound wave release is considered to be a more important source of IG wave on the gentle slope (List, 1992; Janssen et al., 2003). While for the steep slope, the time-varying breakpoint mechanism is considered to be the dominant mechanism for the generation of the IG wave (Battjes et al., 2004; Baldock et al., 2012). Many reefs have very steep slopes with some reef faces even being close to vertical (Gourlay, 1996b). Therefore in many field observations (Pomeroy et al., 2012a; Becker et al., 2016) and experiments (Buckley et al., 2018), IG waves on the reef flat are linked to the time variation of the wave breakpoint. In the surf zone, the wave breakpoint mechanism is also found working against the incident bound IG wave (Pequignet el al., 2014).

Although the IG wave on the reef flat is also damped by the roughness of the reef, the bottom friction has a much greater effect on the short waves than the IG waves (Pomeroy et al., 2012a). The IG wave has a bore-like wave shape (Gawehn et al., 2016). Due to the high propagation speed, the huge inertial forces at the front of the IG wave can cause extensive damage to coastal structures. For example, in the Okinawa islands of southern Japan, seawall, roads and houses sheltered by reef were found damaged by bore-like floods with 10-minutes intervals (Nakaza et al., 1991). During Typhoon Haiyan in 2013, video footage captured serious destruction to a Philippine town by fast-moving bore (Roeber and Bricker., 2015). When the frequencies of the IG wave are close to the natural frequencies of the water body on the reef flat, resonant amplification is possible and the coastal flooding potential increases (Cheriton et al., 2016; Gawehn et al., 2016). The IG wave can also lead to moored ship motions (Van Dongeren et al., 2016) and large resonance (Gao et al., 2019) for the reef-fringed harbors.

Besides the wave breaking, the infragravity wave is also influenced by the reef-fringed shoreline. On the platform reef, wave and current can escape to the sea through the end of the reef flat or lagoon. However, on the fringing reef, infragravity wave will be reflected by the shoreline and then propagate to the open sea or trapped on the reef flat. In order to assess the influence of the shoreline, comparison on the reef hydrodynamics between fringing reef and platform reef is needed. Based on which, an engineering solution that meets specific engineering, ecological criteria may be developed to ameliorate the coastal erosion and flooding.

This paper presents a two-dimensional laboratory experiment to investigate the hydrodynamic processes on an idealized reef under irregular wave conditions. Two different reef profiles are considered: a platform reef and a fringing reef. The generation and propagation of the IG wave on the reef flat are analyzed based on measurements of water surface elevation and flow velocity at 15 locations along the wave flume and the changes in the wave conditions on the reef flat caused by the shoreline are discussed. The paper is organized as below:

Commented [A2]: *Reviewer 2:*
Line 73-76:
Similarly, may also refer to Nakaza and Hino (1991) and Nakaza et al (1991) on this subject.
- *Nakaza, E. and Hino, M. (1991), "Bore-like surf beat in a reef zone caused by wave groups of incident short period waves", Fluid Dynamics Research, 7, 89-100.*
- *Nakaza, E., Tsukayama, S., and Hino, M., (1991), "Bore-like surf beat on reef coasts", Proc., 22nd Int. Conf. Coastal Eng., ASCE, Reston, Va., 743–756.*

Response:
References are added.

the experiment setup is introduced in section 2; the wave propagation and the generation of the IG wave are presented in section 3; the influences of reef-fringed shoreline are discussed in sections 4 and 5 followed by conclusions in section 6.

2. Experiment setup

Laboratory experiments were carried out in the State Key Laboratory of Coastal and Offshore Engineering, Dalian University of Technology, Dalian. The flume is 60 m long, 4 m wide and 2.5 m depth. Zhu et al. (2018) detailed the set of wave flume and the scaled physical models of the reef in regular wave tests. Here these physical models were further used under the irregular wave conditions. The reef model consisted of a steep reef-face with a slope of 1:1 and a horizontal reef flat of 8.6 m long. The reef face and reef flat were built by smooth sand-cement grout, a relatively smooth and impervious surface. The process of wave run-up on the shoreline is not taken into account, therefore the reef-fringed shoreline is adopted as a vertical structure which is 7.2 m away from the reef-edge. Without the shoreline, the reef model is corresponding to a platform reef. Fig. 1 shows the sketch of reef profile and measuring instrument arrangement. Fifteen capacitance wave gauges (TWG-600) and four high resolution acoustic velocity meters (Vectrino) were installed to measure the wave surface elevation and velocity. Locations of wave gauges (G1-G15) and velocity meters (V1-V4) are shown in Fig. 1. The measuring accuracy of the wave gauge is ±0.1 mm. The measuring accuracy of the velocity meter is ±0.5% of the measured value. The sampling rate of 50 Hz was used for all wave gauges and velocity meters.

Incident irregular waves were generated using the JONWSAP spectrum. The model test scale is taken as 1:25. The submergence water depths on the reef flat h_r and incident wave conditions tested in the experiments are listed in Table 1. In total 24 different wave conditions were tested in the experiment. Each test was repeated at least 3 times.

Commented [A3]: *Reviewer 2:*
Line 104-105:
Is it really necessary to state manufacturing country of the instruments?
Response:
Manufacturing country of the instrument is deleted.

Commented [A4]: *Reviewer 2:*
Figure 1 and Line 106:
- *G1-15 and V1-4 needs to be defined/identified (as location of wave gauges and velocity meters) either as annotation on the Figure or in the text (Line #106) where the figure is first referred to.*
- *Caption of Figure 1 (below) unnecessarily repeats the same information twice; and needs to be revised: "Fig. 1. Measuring instrument arrangement and the reef model. (a) Measuring instrument arrangement; (b) Reef model."*

Response:
Revised.

Commented [A5]: *Reviewer 1:*
In line 104 and 105, what's the instrument accuracy?
Response:
The instrument accuracy is added in the revised manuscript.
The measurement accuracy of the wave gauge is ±0.1 mm.
The measurement accuracy of the velocity meter is ±0.5% of the measured value.

3. Generation and propagation of IG wave

The frequency of infragravity wave is commonly taken as from 0.004Hz to 0.04Hz. In the experiment, the model test scale is 1:25, so the corresponding frequency range of IG wave is 0.02-0.2 Hz. The wave surface elevation measured by the wave gauge is η. The average wave set-up $\bar{\eta}$ the rise of water level averaged on the whole acquisition time. The IG component η_{IG} and SS component η_{SS} were filtered based on their frequency ranges.

The wave envelope η_{env} of the incident wave group was calculated based on the Hilbert transform (Janssen et al., 2003):

$$\eta_{\mathrm{env}} = \left|\eta_{\mathrm{SS}} + i\Gamma(\eta_{\mathrm{SS}})\right| \tag{1}$$

where $\Gamma(\ldots)$ denotes the Hilbert transform operator $\Gamma(f(t)) = \int f(t)\mathrm{e}^{-iwt}\mathrm{d}t$. The characteristic spectral wave heights of the IG wave and SS wave were calculated as

$$H_{\mathrm{IG}} = 4\sqrt{\int_{0.02}^{0.2} S_f df} \tag{2}$$

$$H_{\mathrm{SS}} = 4\sqrt{\int_{0.2} S_f df} \tag{3}$$

where S_f is the wave spectral density computed from the wave surface elevation with a segment length of 16384 samples. The characteristic spectral wave height of the incident wave was calculated by the spectral density $S_{f,\mathrm{in}}$ of the incident irregular wave:

$$H_{\mathrm{in}} = 4\sqrt{\int S_{f,\mathrm{in}} df} \tag{4}$$

The characteristic wave heights and the wave set-up $\bar{\eta}$ used the average values of repeated tests. The deviation from the average is calculated by the relative standard deviations (RSD):

$$\mathrm{RSD} = \sqrt{\frac{\sum_{i=1}^{n}(x_i - \bar{x})^2}{n-1}} / \bar{x} \tag{5}$$

where $\bar{x}$ is the average value. The relative standard deviations of the characteristic wave height and the wave set-up at G15 are shown in Table 2. The small values of RSD indicate good test repeatability under different

Commented [A6]: *Reviewer 1:*
In line 118, what's value of gama ?
Response:
Γ denotes the Hilbert transform. This operator applies a frequency independent phase shift of π/2.
$\Gamma(f(t)) = \int f(t)\mathrm{e}^{-iwt}\mathrm{d}t$
This is explained in the revised manuscript.

wave conditions.

In this experiment, the incoming wave (propagating landwards) and outgoing wave (propagating seawards) are separated based on the signals measured from the wave gauges and the velocity meters at the same position (V1-V4 in Fig. 1) in a way similar to that of Buckley et al.'s (2015).

The incident wave envelope η_{env}, filtered wave surface elevations of IG component η_{IG} and SS component η_{SS} are shown in Fig. 2. When the incident wave (Fig. 2a) approaches the reef edge (Fig. 2b), the rapid decrease of the water depth leads to the strong wave deformation and violent wave breaking, then the IG wave is observed on the reef flat (G7-G15). The wave surfaces of SS wave and IG wave have bore-like shapes. As shown in Fig. 2(b), the wave surface of IG wave on the reef flat is in phase with the SS wave group, which is evidence that the IG wave is generated by the time-varying breaking point mechanism (Symonds et al., 1982; Pomeroy et al., 2012a).

Wave spectral densities S_f of different wave gauges are shown in Fig. 3 with the dotted line indicating the spectral densities of incident wave envelope η_{env}. The SS wave is dominant in the incident wave. As waves break on the reef edge at G7, the SS wave energy decreases significantly due to the wave breaking and the IG wave is generated. The frequency of the IG wave mainly depends on the incident wave envelope as the time-varying breakpoint mechanism is dominant in this experiment. Out of the surf zone (G15), the IG wave is dominant, especially for the fringing reef.

Schäffer (1993) found that the IG wave height has a positive correlation with the wave height variation of the incident wave group. For the irregular wave, the wave height variation of the wave group can be revealed by the standard deviations σ_{env} of η_{env}. Fig. 4 shows the relationship between σ_{env} and the IG wave height H_{IG} on the reef flat at G15. A strong linear correlation is clearly observed between σ_{env} and the IG wave height H_{IG}. Due to that the increase of the wave period may lead to an increase in the wave groupiness

(Karunarathna et al., 2005), σ_{env} for significant period $T_s = 2.0$ s, is a slightly larger than that for $T_s = 1.5$ s. Therefore, the IG wave height H_{IG} on the reef flat is larger in general when $T_s = 2.0$ s.

Based on the incident wave envelope η_{env} and the IG wave surface η_{IG} at different measuring points, the cross correlation $R_{eI}(\tau)$ can be calculated (Janssen et al., 2003) as

$$R_{eI}(\tau) = \frac{\langle \eta_{env}(t)\eta_{IG}(t+\tau) \rangle}{\sigma_{env}\sigma_{IG}} \quad (6)$$

where $\langle ... \rangle$ is the time averaging operator, τ is the time lag between η_{env} and η_{IG}, σ_{env} and σ_{IG} are standard deviations of η_{env} and η_{IG} respectively. Fig. 5 shows the cross correlation $R_{eI}(\tau)$ between the incident wave envelope η_{env} and the IG wave surface η_{IG} at different measuring points. The generation and propagation of the IG waves are revealed by the color map of $R_{eI}(\tau)$ under different time lags τ. The dotted lines in Fig. 5(b) are the theoretical path of the IG waves. Based on the theoretical speed of the incident wave group, the theoretical path of bound IG wave in the incident wave group is shown as Path 1. Paths 2-6 are the theoretical path of free IG wave, which is calculated by the wave velocity related to the local water depth. Due to that the bound IG wave in the incident wave group is small, no obvious negative correlation is found along Path 1.

When waves propagate onto the reef flat, the breaking of the incident wave group generates IG waves. Therefore on the reef flat (x >1.8 m), clear positive correlation is observed (Path 3). The wave breaking of the wave group can also generate outgoing IG waves, as shown along Path 2 (negative correlation). Previous researches on the time-varying breakpoint mechanism showed that the incoming IG wave is in phase with the wave group and the outgoing IG wave has a phase difference of 180° with the wave group (Baldock et al., 2012; Contardo and Symonds, 2013). The same is found in the results of this experiment, confirming that in this experiment both the incoming and outgoing IG waves are generated by the time-varying breakpoint mechanism. For the fringing reef, the incoming IG wave reflects from shoreline (Path 4). However, the reflected outgoing

Commented [A7]: *Reviewer 1:*
In line 157 Explain the reasons for effect of wave period on HIG ?
Response:
IG wave height has a positive correlation with the wave height variation of the incident wave group (Schäffer, 1993). For the irregular wave, the wave height variation of the wave group can be revealed by the wave groupiness of the incident wave. The increase of the wave period may lead to an increase in the wave groupiness (Karunarathna et al., 2005). Therefore in our experiment, the wave groupiness of the incident wave increases with the increase of the significant wave period, which finally lead to an increase of the IG wave height. This explanation is included in the revised manuscript.

IG waves do not propagate further out to the open sea as Path 6 shows. The possible reason is that the rapid change of the water depth around the reef edge leads to a wave reflection as Path 5 shows. It is worthy noticing that the cross correlation along Path 5 is relatively small.

4. Distributions of wave height and wave set-up on the reef flat

Wave set-up $\bar{\eta}$, IG wave height H_{IG} and SS wave height H_{SS} are nondimensionalized by the wave height of the incident wave height H_{in}. The distributions of $\bar{\eta}/H_{\mathrm{in}}$, $H_{\mathrm{IG}}/H_{\mathrm{in}}$ and $H_{\mathrm{SS}}/H_{\mathrm{in}}$ are shown in Fig. 6. As expected, IG wave height and wave set-up increases in the surf zone. For the platform reef, when the water depth on the reef flat is small ($h_{\mathrm{r}} < 5$ cm), the large values of IG wave height and wave set-up are found at the reef edge (G7). The maximum of the IG wave height may occur at the reef edge as shown in Fig. 6 (d-e). Then the IG wave height decreases rapidly at G8 and increases gradually along the reef flat.

For the platform reef, the wave propagation over the reef edge under different water depths is shown in Fig. 7. When the water depth is small, the wave overtopping on the reef edge generates an obvious increase of the water level. It leads to the large wave set-up and IG wave at G7. As shown in Fig.7(a-c), the high water level at reef edge accelerates the flow propagating landwards and the water level decreases quickly around G8. For the platform reef, the time series of wave surface elevation η and IG wave component η_{IG} at G7 and G8 are shown in Fig. 8. These time series also show a decrease of water level from G7 to G8. Therefore, the wave set-up and IG wave have a rapid decrease around the reef edge. In our experiment, the outer reef flat (G8-G13) is the surf zone. The wave breaking in the surf zone brings the increase of wave set-up and IG wave height (G8-G13). Then the wave set-up and IG wave height tend to be stable (G13-G15). When the water depth increases, there is no obvious wave overtopping over the reef edge, as shown in Fig. 7(d-f). Therefore, the wave set-up and IG wave height increase along the reef flat due to the wave breaking.

Commented [A8]: *Reviewer 1:*
7. In line187, why does IG wave height decrease rapidly at G8?
Response:
This point is taken. This phenomenon is analyzed based on the observation of the wave breaking on the reef edge and the time series of the water surface for different water depths.
The photos of the wave overtopping on the reef edge are included in the revised manuscript. The relevant analysis results in added in paragraph two of Section 4.

For the fringing reef, the reef flat is blocked by the shoreline. Wave overtopping over the reef edge can not generate flow propagating shoreward. Therefore, the rapid decreases of wave set-up and IG wave height cease to occur at the reef edge. The suppression of the wave-induced flow leads to a further rise of the mean water level, as shown in Fig. 6(a-c). The scatters in Fig. 6(d-f) are the separated incoming and outgoing IG wave heights. The vertical shoreline in this experiment leads to a complete reflection of the incoming IG wave. The IG wave is larger than that for the platform reef. For example, as shown in Fig. 6(d-f), the relative IG wave height H_{IG}/H_{in} is about 0.2 on the platform reef. For the fringing reef, the relative IG wave height H_{IG}/H_{in} in front of the shoreline is about 0.6, increases by a factor of 3. The scatters in Fig. 6(d-f) are the separated IG wave heights of the incoming and outgoing IG waves. It can be seen that the vertical shoreline in this experiment leads to a complete reflection of the incoming IG wave.

As shown in Fig. 6(g-i), the SS wave height decreases rapidly in the surf zone. Outside the surf zone, the SS wave height is almost constant as a result of the smooth reef surface in the experiment. For the fringing reef, the submergence depth $(\bar{\eta}_r + h_r)$ increases, which leads to a small increase of the SS wave height.

5. Wave heights in front of the shoreline

The wave heights in front of the shoreline are shown in Fig. 9. The horizontal axis is the non-dimensional submergence depth on the reef flat $((\bar{\eta}_r + h_r)/H_{in})$, where $\bar{\eta}_r$ is the wave set-up at G15. Fig. 9(a) shows the relative SS wave height H_{SS}/H_{in} in front of the shoreline (G15). It can be seen that the SS wave height is proportional to the water depth, as a result of the SS wave heights being limited by the submergence depth on the reef flat. For the platform reef, the ratio γ of the SS wave height H_{ss} and submergence depth $(\bar{\eta}_r + h_r)$ in the inner surf zone ranges from 0.50 to 0.67. For the fringing reef, the wave reflection and slamming on the

Commented [A9]: *Reviewer 1:*
2) Some results are obvious. Of course, the IG will higher on the fringing reef, but the main reason is that water is blocked by the shoreline, which will lead to higher wave setup. Can this kind of setup be considered as IG? It should be discussed.
Response:
The mean water level on the reef flat is composed of two parts: (1) average wave set-up: the rise of water level averaged on the whole acquisition time; (2) IG wave: the oscillation of the wave set-up averaged on the SS wave periods.
We agree with the reviewer that on the fringing reef, the water is blocked by the shoreline, which leads to higher average wave set-up (as shown in Fig. 6a-Fig.6c). However, this kind of setup is not considered here as caused by IG wave. The setup that have been attributed to IG wave is the reflection of IG wave from the shoreline as discussed in section 4 and 5. The relevant discussion is added in the revised manuscript to make this point clear.

Commented [A10]: *Reviewer 2:*
Line 207-208
" ... For the fringing reef, the SS wave height has a small increase."
Please discuss the reason. Larger wave setup (in the case of a fringing reef), which subsequently provides a larger total water depth (hr + setup), is responsible for allowing larger (near-)equilibrium SS wave height near the shoreline.
Response:
The SS wave height on the reef flat is controlled by the water depth. For the fringing reef, the larger submergence depth $(\bar{\eta}_r + h_r)$ is responsible for the larger SS wave height. This is discuss in section 4.

vertical shoreline generate larger γ ranged from 0.56 to 0.75.

Fig. 9(b) shows the relative IG wave height $H_{\mathrm{IG}}/H_{\mathrm{in}}$ in front of the shoreline at G15. For the fringing reef, the IG wave height has significant increase by a factor of 2-3. Therefore, the IG wave heights in front of the shoreline remain quite high as the relative IG wave height is from 0.49-0.68 under different wave conditions. The obvious reason for the significant increase of the IG wave height is the perfect wave reflection from the shoreline. With a gentle shoreline, the IG wave height will decrease due to the decrease of the wave reflection. For the fringing reef, the wave heights of the separated incoming IG wave at G15 are shown in Fig. 9(b). It can be seen that the incoming IG wave heights are also larger than the IG wave heights for the platform reef. Fig. 9(c) shows the relative IG wave heights $H_{\mathrm{IG}}/H_{\mathrm{in}}$ at G6. The IG waves at G6 are considered as the outgoing IG waves generated in the surf zone (Path 2 in Fig. 5). For the fringing reef, the outgoing IG wave heights at G6 also increase as shown in Fig. 9(c). These phenomena indicate that with the shoreline, the wave breaking in the surf zone may generate larger outgoing (Path 2) and incoming (Path 1) IG waves. Fig. 10 shows the photos of the wave breaking around the reef edge at the same moment for the platform reef and fringing reef. It can be seen that with the shoreline, the wave generated flow can't flow out of the reef flat and the high water level on the reef flat generates strong backflow (Zhu et al., 2018) which in turn induces a more violent wave breaking. As a consequence, for the fringing reef, the outgoing (Path 2) and incoming (Path 1) IG waves generated in the surf zone may increase.

The ratio of the IG wave height and SS wave height $H_{\mathrm{IG}}/H_{\mathrm{SS}}$ at G15 are shown in Fig. 9(d). When submergence depth decreases, IG wave plays a more important role on the reef flat. For the fringing reef, the values of $H_{\mathrm{IG}}/H_{\mathrm{SS}}$ are more than 1 in general, which indicates IG wave dominance under all submergence depth. In the case of the real reef, the bottom friction has a much greater effect on damping the short waves compared to the IG waves (Pomeroy et al., 2012a) and the SS wave in front of the shoreline may become even

smaller.

For the fringing reef, Comparisons of IG wave height between our experiment and previous studies are shown in Table A1. Due to the steep reef face, the vertical shoreline and smooth surface, our experiment have the largest relative IG wave heights (0.49-0.68). The field observations have smaller IG wave height on the reef flat than the laboratory experiments with smooth surface.

In field observations (Pomeroy et al., 2012a; Gawehn et al., 2016), the IG wave was found to increase notably with the increase of the submergence depth. They attribute this to the bottom friction or reef resonance. When the water depth increases, the wave energy dissipation induced by the bottom friction decreases (Pomeroy et al., 2012a). Larger water depth on the reef flat also increases the probability of resonance (Gawehn et al., 2016). When water depth increases, the resonance and the decrease of the wave energy dissipation lead to a large IG wave heights on the reef flat. However, when the bottom friction is small, this proportional relationship will disappear. For example, in Beetham et al.'s (2015) field observation, the IG wave height is minimally affected by the water depth. Nwogu and Demirbilek's (2010) and Yao et al.'s (2020) laboratory experiment results are reanalyzed in dimensionless forms, as shown in Fig. 11. Different from field observations, the IG wave height decreases with the increase of the submergence depth in our experiment and Yao et al.'s (2020) experiment. The efficiency of the breakpoint mechanism decreasing as the water depth over the reef increases, which results in a decrease generation of IG wave in the surf zone. When the bottom friction is small enough to be neglected, the wave breaking mechanism will control an opposite relationship between IG wave height and water depth. Noticeably, Nwogu and Demirbilek's (2010) experiments show a different trend due to the obvious reef resonance at large water depth. Therefore, when water depth increases, the IG wave height is influenced by these three factors which act counter to each other. However, the efficiency of the breakpoint mechanism seems to be a less important factor than bottom friction and resonance.

Commented [A11]: *Reviewer 2:*
Over the past decade, a number of studies investigated the subject of IG waves on reefs (some already cited in the manuscript; and few others which I listed in my review comments). However, except for a few lines (L#219-222), the authors did not provide any comparison between data and conclusions from the present experiment and those of the previous studies. I suggest a revision of Sections 3-5 to include a comparison (ideally quantitative) with previous studies, especially previous laboratory studies. I believe this would greatly enhance this paper.

Response:
We agree with this comment completely. Field observations and laboratory experiments are compared in Table A1. The IG wave heights measured in Nwogu's (2010) and Yao's (2020) laboratory experiment results are also reanalyzed in dimensionless form and shown in Fig. 11.
Detailed discussion and comparison are added in Section 5 in the revised manuscript.

6. Conclusions

In order to investigate the hydrodynamic processes on an idealized reef under irregular wave conditions, a two-dimensional experiment is carried out. Strong IG waves are generated on the reef flat by the time-varying breakpoint mechanism. The IG wave height on the reef flat is proportional to the standard deviations σ_{env} of the incident wave envelope η_{env}. The larger significant period T_{s} of the incident wave leads to a larger IG wave height on the reef flat.

Different with the field observations, the IG wave height is found to decrease slightly with the increase of the submergence depth. The efficiency of the breakpoint mechanism decreasing as the water depth over the reef increases, which results in a reduction of IG wave generated inside the surf zone. In the case of the real reef, bottom stress, reef resonance and wave breaking all have influence on the IG wave height. However, the efficiency of the breakpoint mechanism seems to be a less important factor.

For the fringing reef, the wave set-up, SS wave height and IG wave height on the reef flat all show varying degrees of increase. IG wave height can be even three times larger in the presence of the vertical shoreline. Two reasons are responsible for this increase of the IG wave: (1) the superposition of incoming IG wave and reflected IG wave and (2) more violent wave breaking in the surf zone. Because that the SS wave height is more strongly limited by the shallow water depth on the reef flat, the SS wave in front of the shoreline plays a much less important role than the IG wave does. The IG wave should be considered as the most important factor especially in the fringing reef system. The relative large size of the IG wave heights on the fringing reef and on the platform reef is observed under the specific setup of the experiment such as a vertical wall, smooth surface and steep reef face. Must more tests will also be required to assess fully the effects of the distance and front slope on IG wave propagation to develop a more general relationship between the relative wave height and these controlling parameters.

Commented [A12]: *Reviewer 1:*
3) Another main finding of this paper is 'The IG wave height can be as three times larger on the fringing reef than that on the platform reef.' However this is a conclusion under a certain condition, including a vertical wall, 1:1 front slope, and 7.2m distance. Once the condition changes, it is also 3 times? It is not a common conclusion. It is suggested to author that more tests can be done to analyze the effects of distance, front slope on IG. Then a relationship can be obtained. It is more meaningful.
Response:
We agree with the reviewer that the relative size of the IG wave heights on the fringing reef and on the platform reef is observed under the specific setup of the experiment such as a vertical wall, smooth surface and steep reef face. Must more tests will also be required to assess fully the effects of the distance and front slope on IG wave propagation to develop a more general relationship between the relative wave height and these controlling parameters. These points are added in the conclusion of revised manuscript.

CRediT authorship contribution statement

Gancheng Zhu: Investigation, Methodology, Writing - original draft, Formal analysis. **Bing Ren**: Validation, Methodology, Funding acquisition, Supervision, Writing - review & editing. **Dong Ping**: Supervision, Writing - review & editing, Formal analysis. **Guoyu Wang**: Writing - review & editing, Formal analysis. **Weidong Chen**: Formal analysis.

Declaration of competing interest

The authors declare that they have no known competing financial interests or personal relationships that could have appeared to influence the work reported in this paper.

Acknowledgments

This work was supported by the National Natural Science Foundation of China under Grant No. 51979028.

Appendix A

Field observations and laboratory experiments are compared with our experiment results in Table A1. The IG wave heights mearsued in thes studies are transformed to the characteristic wave height H_{IG}.

References

Baldock, T.E., 2012. Dissipation of incident forced long waves in the surf zone-Implications for the concept of ‘‘bound’’ wave release at short wave breaking. Coast. Eng. 60, 276–285. https://doi.org/10.1016/j.coastaleng.2011.11.002.

Baldock, T.E., Shabani, B., Callaghan, D.P., Hu, Z., Mumby, P.J., 2020. Two-dimensional modelling of wave dynamics and wave forces on fringing coral reefs. Coast. Eng. 155, 103594. https://doi.org/10.1016/j.coastaleng.2019.103594.

Battjes, J.A., Bakkenes, H.J., Janssen, T.T., van Dongeren, A.R., 2004. Shoaling of sub- harmonic gravity waves. J. Geophys. Res. 109(C2). http://dx.doi.org/10.1029/ 2003JC001863.

Becker, J.M., Merrifield, M.A., Ford, M., 2014. Water level effects on breaking wave setup for Pacific Island fringing reefs. J. Geophys. Res.-Oceans 119, 914–932. https://doi.org/10.1002/2013JC009373.

Becker, J.M., Merrifield, M.A., Yoon, H., 2016. Infragravity waves on fringing reefs in the tropical Pacific: Dynamic setup. J. Geophys. Res.-Oceans 121, 3010–3028. https://doi.org/10.1002/2015JC011516.

Beetham, E., Kench, P., O'Callaghan, J., and Popinet, S., 2016, Wave transformation and shoreline water level on Funafuti Atoll, Tuvalu. J. Geophys. Res. Oceans 121, 311–326. https://doi.org/10.1002/2015JC011246.

Buckley, M.L., Lowe, R.J., Hansen, J.E., Van Dongeren, A.R., 2015. Dynamics of wave setup over a steeply sloping fringing reef. J. Phys. Oceanogr. 45 (12), 3005-3023. https://doi.org/10.1175/JPO-D-15-0067.1.

Buckley, M.L., Lowe, R.J., Hansen, J.E., Van Dongeren, A.R., 2016. Wave setup over a fringing reef with large bottom roughness. J. Phys. Oceanogr. 46 (8), 2317-2333. https://doi.org/10.1175/JPO-D-15-0148.1.

Buckley, M.L., Lowe, R.J., Hansen, J.E., Van Dongeren, A.R., Storlazzi, C.D., 2018. Mechanisms of wave-driven water level variability on reef-fringed coastlines. J. Geophys. Res.-Oceans 123 (5), 3811-3831. https://doi.org/10.1029/2018JC013933.

Cabioch, G., Davies, P., Done, T., Gischler, E., Macintyre, I. G., Wood, R. and Woodroffe, C., 2010. Encyclopedia of modern coral reefs: structure, form and process. Springer Science & Business Media.

Cheriton, O., Storlazzi, C., Rosenberger, K., 2016. Observations of wave transformation over a fringing coral reef and the importance of low-frequency waves and offshore water levels to runup, overwash, and coastal flooding. J. Geophys. Res. Oceans 121 (5), 3121-3140. https://doi.org//10.1002/2015JC011231.

Contardo, S., Symonds, G., 2013. Infragravity response to variable wave forcing in the nearshore. J. Geophys. Res.-Oceans 118 (12), 7095-7106. https://doi.org/10.1002/2013JC009430.

Ferrario, F., Beck, M. W., Storlazzi, C. D., Micheli, F., Shepard, C.C, Airoldi, L., 2014. The effectiveness of coral reefs for coastal hazard risk reduction and adaptation. Nat. Commun. 5, 3794. https://doi.org/10.1038/ncomms4794.

Franklin, G., Mariño-Tapia, I., Torres-Freyermuth, A., 2013. Effects of reef roughness on wave setup and surf zone currents. J. Coast. Res. 65 (sp2), 2005-2011. https://doi.org/10.2112/SI65-339.1.

Gao, J., Zhou, X., Zhou, L., Zang, J., Chen, H., 2019. Numerical investigation on effects of fringing reefs on low-frequency oscillations within a harbor. Ocean Eng. 172, 86-95. https://doi.org/10.1016/j.oceaneng.2018.11.048.

Gawehn, M., Van Dongeren, A., Van Rooijen, A., Storlazzi, C.D., Cheriton, O.M., Reniers, A., 2016. Identification and classification of very low frequency waves on a coral reef flat. J. Geophys. Res.-Oceans 121 (10): 7560-7574. https://doi.org/10.1002/2016JC011834.

Gerritsen, F., 1980. Wave attenuation and wave set-up on a coastal reef. Coastal Engineering 1980, 444-461.

Gourlay, M.R., 1994. Wave transformation on a coral reef. Coast. Eng. 23(1-2), 17-42. https://doi.org/10.1016/0378-3839(94)90013-2.

Gourlay, M.R., 1996a. Wave set-up on coral reefs. 1. Set-up and wave-generated flow on an idealised two dimensional horizontal reef. Coast. Eng. 27, 161-193. https://doi.org/10.1016/0378-3839(96)00008-7.

Gourlay, M.R., 1996b. Wave set-up on coral reefs. 2. Set-up on reefs with various profiles. Coast. Eng. 28, 17-53. https://doi.org/10.1016/0378-3839(96)00009-9.

Janssen, T.T., Battjes, J.A., Van Dongeren, A.R., 2003. Long waves induced by short-wave groups over a sloping bottom. J. Geophys. Res.-Oceans. 108 (C8), 3252. https://doi.org/10.1029/2002JC001515.

Karunarathna, H., Chadwick, A., Lawrence, J., 2005. Numerical experiments of swash oscillations on steep and gentle beaches. Coast. Eng. 52 (6), 497-511. https://doi.org/10.1016/j.coastaleng.2005.02.003.

Longuet-Higgins, M.S., Stewart, R.W., 1962. Radiation stress and mass transport in gravity waves, with application to surf beats. J. Fluid Mech. 13, 481–504. https://doi.org/10.1017/S0022112062000877.

Lowe, R.J., Falter, J.L., Bandet, M.D., Pawlak, G., Atkinson, M.J., Monismith, S.G., Koseff, J.R., 2005. Spectral wave dissipation over a barrier reef. J. Geophys. Res.-Oceans., 110(C4). https://doi.org/10.1029/2004JC002711.

List, J.H., 1992. A model for the generation of 2-dimensional surf beat. J. Geophys. Res.-Oceans 97, 5623–5635. https://doi.org/10.1029/91JC03147.

Liu, Y., Li, S., 2018. Variation of wave groupiness across a fringing reef. J. Waterw. Port Coast. Ocean Eng., 144 (6), 04018022. https://10.1061/(ASCE)WW.1943-5460.0000475.

Munk, W.H., Sargent, M.C., 1948. Adjustment of Bikini Atoll to ocean waves. Trans. Am. Geophys. Union 29, 855–860. https://doi.org/10.1029/TR029i006p00855.

Nakaza, E., Tsukayama, S., Hino, M., 1991. Bore-like surf beat on reef coasts. Coastal Engineering 1990. 743-756.

Nwogu, O., Demirbilek, Z., 2010. Infragravity wave motions and runup over shallow fringing reefs. Journal of waterway, port, coastal, and ocean engineering. 136(6), 295-305. https://doi.org/10.1061/(ASCE)WW.1943-5460.0000050.

Péquignet, A., Becker, J.M., Merrifield, M.A., Aucan, J., 2009. Forcing of resonant modes on a fringing reef during tropical storm Man-Yi. Geophys. Res. Lett. 36, L03607. https://doi.org/10.1029/2008GL036259.

Pequignet, A., Becker, J., and Merrifield, M., 2014. Energy transfer between wind waves and low-frequency oscillations on a fringing reef, Ipan, Guam. J. Geophys. Res. Oceans, 119, 6709–6724. https://doi.org//10.1002/2014JC010179.

Poate, T., Masselink, G., Austin, M.J., Inch, K., Dickson, M., and McCall, R., 2020. Infragravity wave

generation on shore platforms: Bound long wave versus breakpoint forcing. Geomorphology, 350, 106880.

Pomeroy, A., Lowe, R.J., Symonds, G., Van Dongeren, A.R., and Moore, C., 2012a. The dynamics of infragravity wave transformation over a fringing reef. J. Geophys. Res. 117, C11022. https://doi.org/10.1029/2012JC008310.

Pomeroy, A., Van Dongeren, A., Lowe, R., van Thiel de Vries, J. and Rovelvink, J., 2012b. Low frequency wave resonance in fringing reef environments. Coastal Eng. Proc. (33), 25-25. https://doi.org/10.9753/icce.v33.currents.25.

Roeber, V., Bricker, J.D., 2015. Destructive tsunami-like wave generated by surf beat over a coral reef during Typhoon Haiyan. Nat. Commun. 6, 7854. https://doi.org/10.1038/ncomms8854.

Schäffer, H.A., 1993. Infragravity waves induced by short-wave groups. J. Fluid Mech. 247, 551-588. https://doi.org/10.1017/S0022112093000564.

Symonds, G., Huntley, D.A., and Bowen, A.J., 1982. Two-dimensional surf beat: Long wave generation by a time-varying breakpoint. J. Geophys. Res. 87, 492–498. https://doi.org/10.1029/JC087iC01p00492.

Tait, R.J., 1972. Wave set-up on coral reefs. J. Geophys. Res. 77, 2207-2211. https://doi.org/10.1029/JC077i012p02207.

Van Dongeren, A., Lowe, R., Pomeroy, A., Trang, D., Roelvink, J., Symonds, G., and Ranasinghe, R., 2013. Numerical modeling of low-frequency wave dynamics over a fringing coral reef. Coast. Eng. 73, 178-190. https://doi.org/10.1016/j.coastaleng.2012.11.004.

Van Dongeren, A., De Jong, M., Van der Lem, C., Van Deyzen, A., Den Bieman, J., 2016. Review of long wave dynamics over reefs and into ports with implication for port operations. J. Mar. Sci. Eng. 4(1), 12. https://doi.org/10.3390/jmse4010012.

Vetter, O., Becker, J.M., Merrifield, M.A., Pequignet, A.C., Aucan, J., Boc, S.J., Pollock, C.E., 2010. Wave

setup over a Pacific Island fringing reef. J. Geophys. Res.-Oceans. 115 (C12). https://doi.org/10.1029/2010JC006455.

Yao, Y., He, W., Du, R., Jiang, C., 2017. Study on wave-induced setup over fringing reefs in the presence of a reef crest. Appl. Ocean Res. 66,164-177. http://doi.org/10.1016/j.apor.2017.06.002.

Yao, Y., Huang, Z., He, W., Monismith, S.G., 2018. Wave-induced setup and wave-driven current over Quasi-2DH reef-lagoon-channel systems. Coast. Eng. 138, 113-125. https://doi.org/10.1016/j.coastaleng.2018.04.009.

Zhu, G, Xia, Y, Ren, B, Wang, G., 2018. The influence of vertical-Wall structure on monochromatic wave propagation characteristics Over the deep-Sea Coral reefs. The 28th International Ocean and Polar Engineering Conference. International Society of Offshore and Polar Engineers.

Zhu, G., Ren, B., Wen, H., Wang, Y., Wang, C., 2019. Analytical and experimental study of wave setup over permeable coral reef. Appl. Ocean Res. 90, 101859. https://doi.org/10.1016/j.apor.2019.101859.

Figure captions

Fig. 1. Experiment set-up. (a) Measuring instrument arrangement; (b) Reef model.

Fig. 2. Wave surface elevations (h_r = 0.05 m, T_s = 2.0 s, H_s = 0.2 m). (a) Incident wave and wave envelope η_{env}; (b) Filtered wave surface at G7; (c) Filtered wave surface at G15.

Fig. 3. Wave spectral densities S_f (h_r = 0.05 m, T_S = 2.0 s, H_S = 0.2 m). (a) Platform reef; (b) Fringing reef.

Fig. 4. Relationship between σ_{env} and the IG wave height H_{IG} on the reef flat (G15).

Fig. 5. Cross correlation $R_{\mathrm{el}}(\tau)$ between the incident wave envelope η_{env} and the IG wave surface η_{IG} (h_r = 0.05 m, T_s = 2.0 s, H_s = 0.2 m). (a) Platform reef; (b) Fringing reef.

Fig. 6. Distributions of the relative wave set-up and relative wave height. (a-c) Wave set-up; (d-f) IG wave height. (g-i) SS wave height.

Fig. 7. Wave propagation over the reef edge for the platform reef (a-c) h_r = 0.00 m, T_s = 1.5 s, H_s = 0.2 m; (d-f) h_r = 0.10 m T_s = 1.5 s, H_s = 0.2 m.

Fig. 8. Wave surface elevations at G7 and G8 for platform reef (h_r = 0.00 m, T_s = 2.0 s, H_s = 0.2 m).

Fig. 9. Relationship between wave height and non-dimensional submergence depth on the reef flat. (a) Relative SS wave height $H_{\mathrm{SS}}/H_{\mathrm{in}}$ at G15; (b) Relative IG wave height $H_{\mathrm{IG}}/H_{\mathrm{in}}$ at G15; (c) Relative IG wave height $H_{\mathrm{IG}}/H_{\mathrm{in}}$ at G6; (d) Ratio of IG wave height and SS wave height $H_{\mathrm{IG}}/H_{\mathrm{SS}}$ at G15.

Fig. 10. Wave breaking around the reef edge. (a) Platform reef; (b) Fringing reef.

Fig. 11. Distribution of IG wave height for different larboratory experiments.

Table captions

Table 1 Water depth on the reef flat and incident wave conditions.

Table 2 Relative standard deviations at G15.

Table A1 Infragravity wave heights in field observations and laboratory experiments

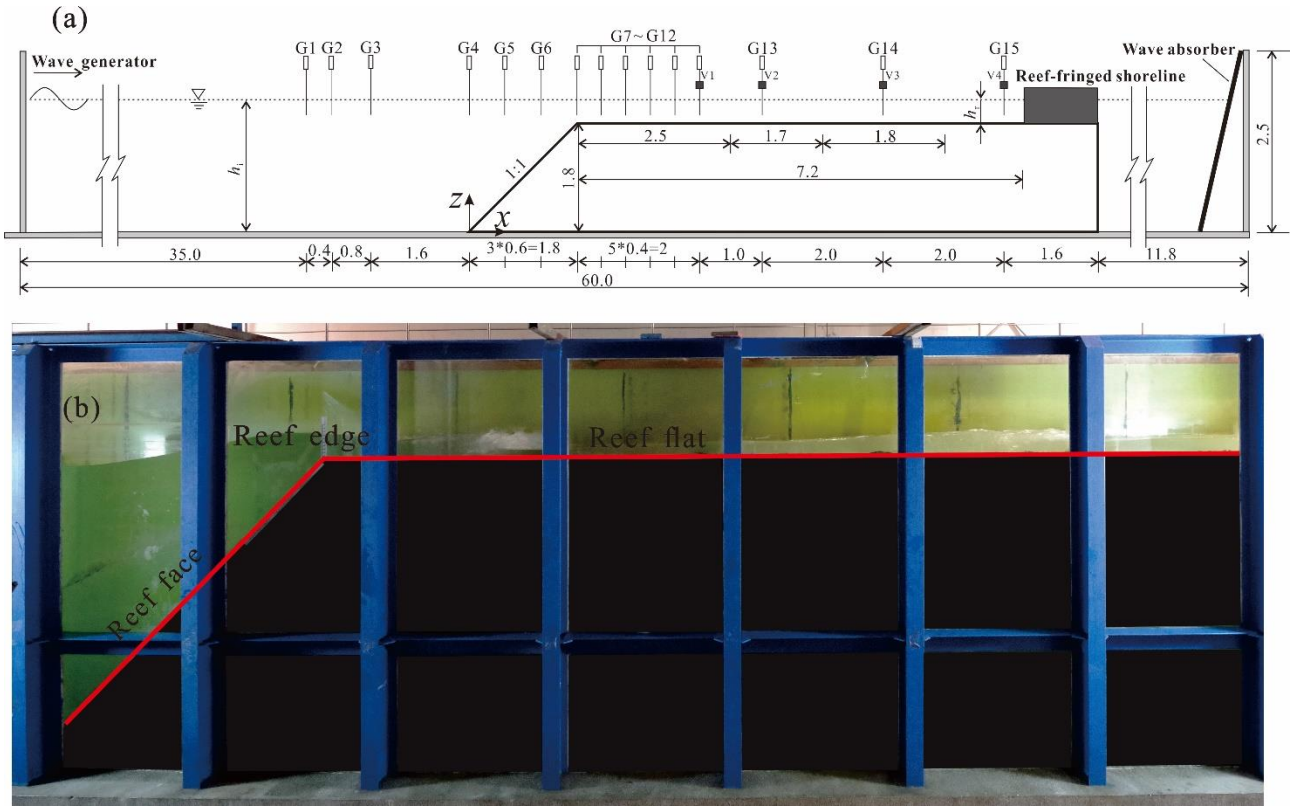

Fig. 1. Experiment set-up. (a) Measuring instrument arrangement; (b) Reef model.

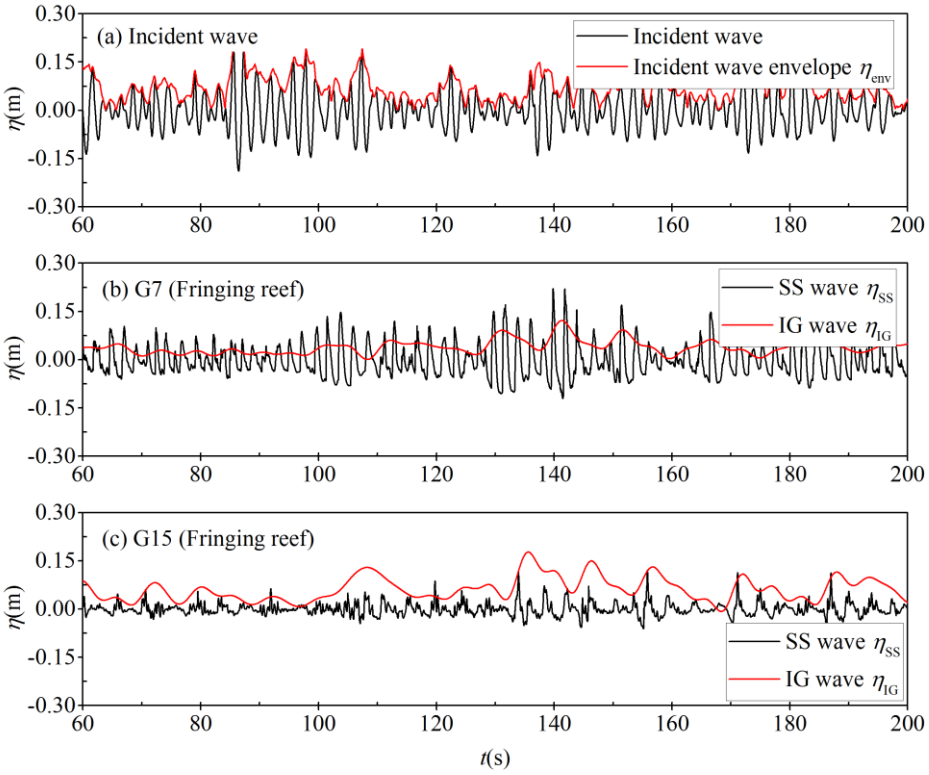

Fig. 2. Wave surface elevations (h_r = 0.05 m, T_s = 2.0 s, H_s = 0.2 m). (a) Incident wave and wave envelope η_{env}; (b) Filtered wave surface at G7; (c) Filtered wave surface at G15.

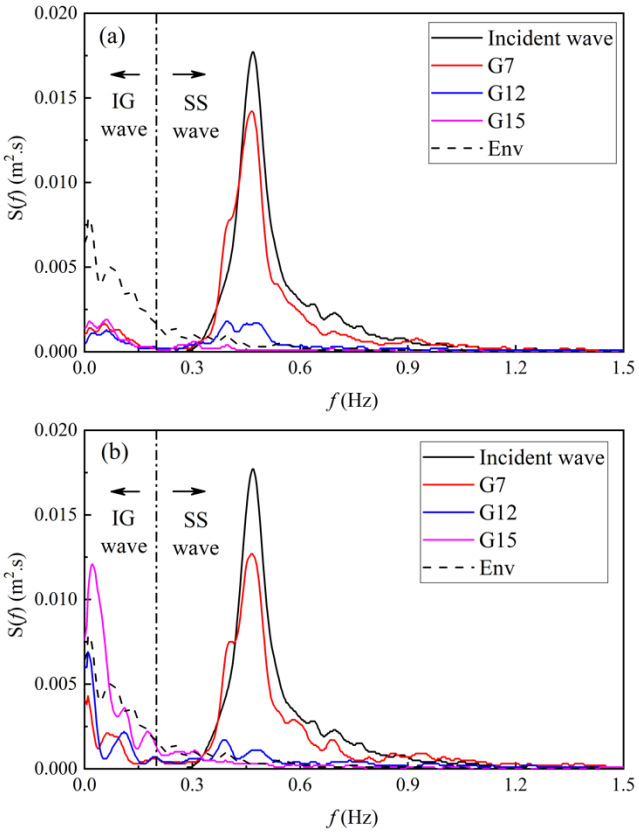

Fig. 3. Wave spectral densities S_f (h_r = 0.05 m, T_s = 2.0 s, H_s = 0.2 m). (a) Platform reef; (b) Fringing reef.

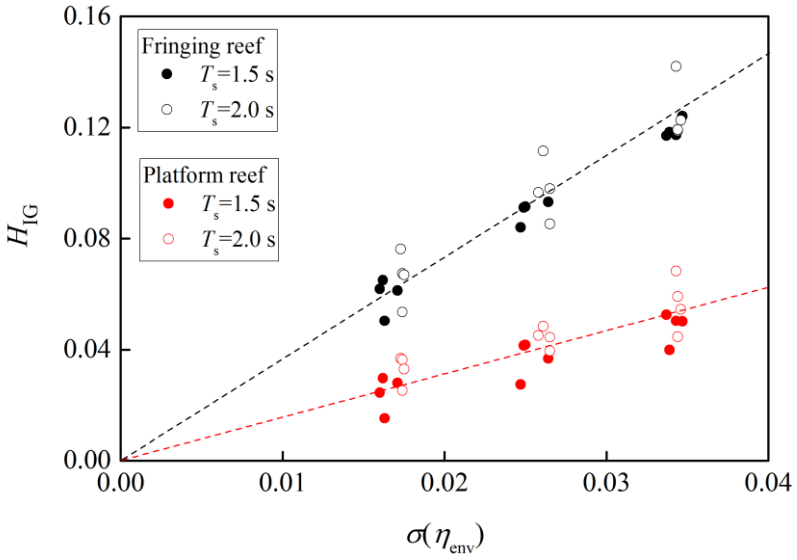

Fig. 4. Relationship between σ_{env} and the IG wave height H_{IG} on the reef flat (G15).

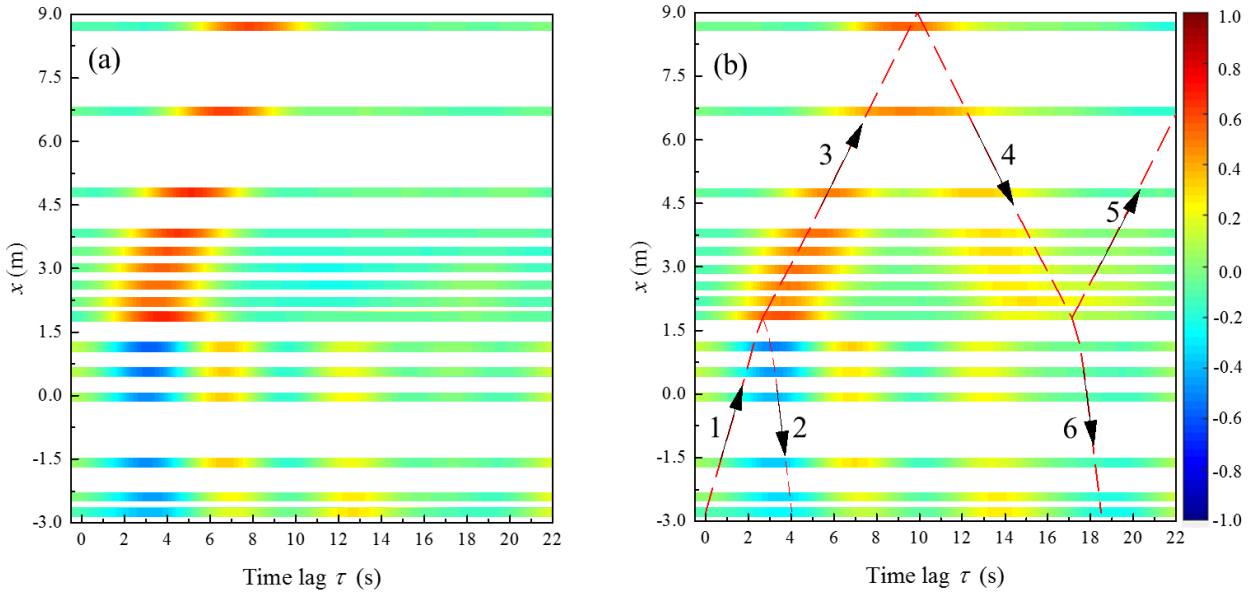

Fig. 5. Cross correlation $R_{\mathrm{eI}}(\tau)$ between the incident wave envelope η_{env} and the IG wave surface η_{IG} (h_{r} = 0.05 m, T_{s} = 2.0 s, H_{s} = 0.2 m). (a) Platform reef; (b) Fringing reef.

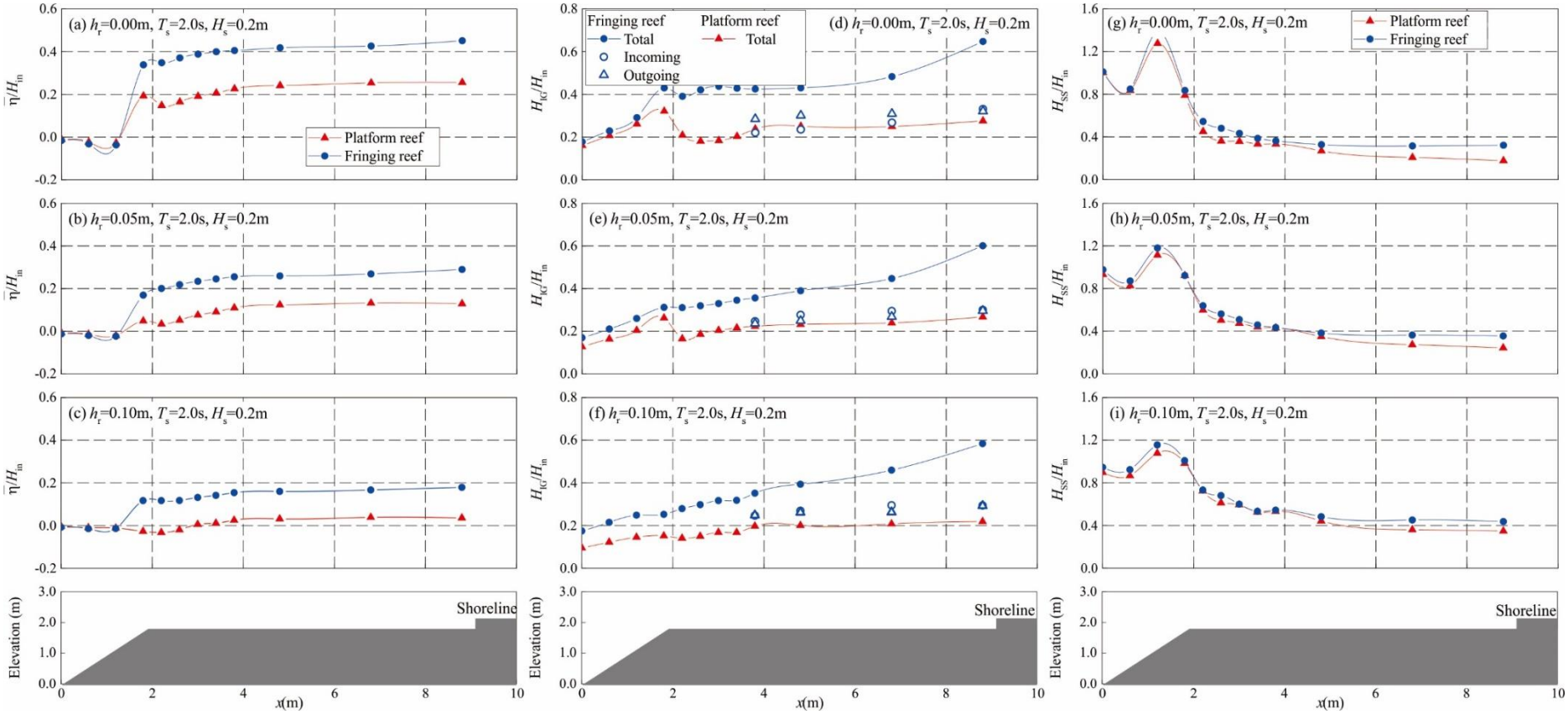

Fig. 6. Distributions of the relative wave set-up and relative wave height. (a-c) Wave set-up; (d-f) IG wave height. (g-i) SS wave height.

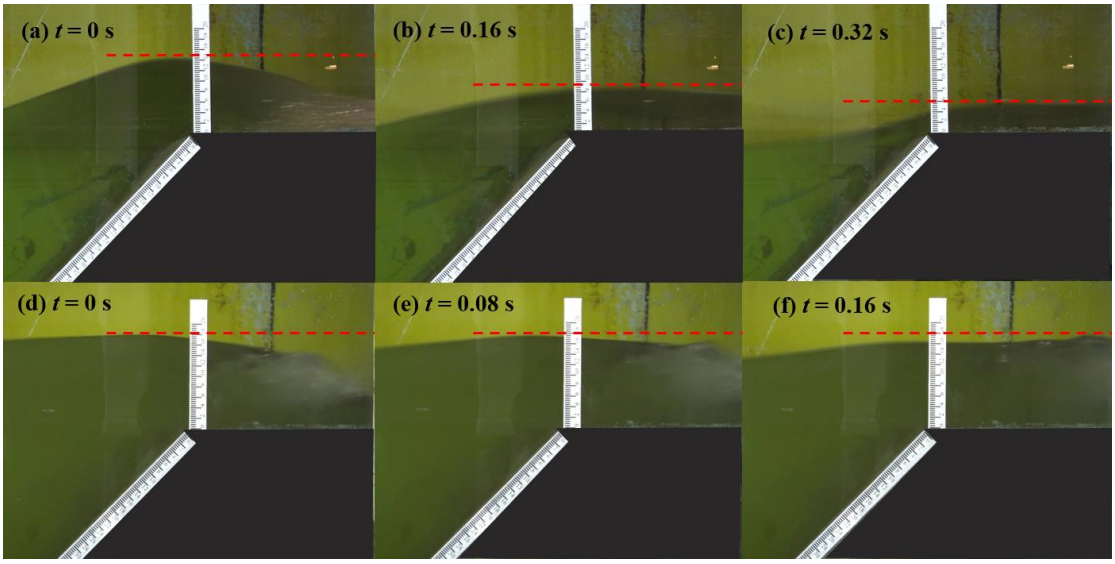

Fig. 7. Wave propagation over the reef edge for the platform reef (a-c) h_r = 0.00 m, T_s = 1.5 s, H_s = 0.2 m; (d-f) h_r = 0.10 m, T_s = 1.5 s, H_s = 0.2 m

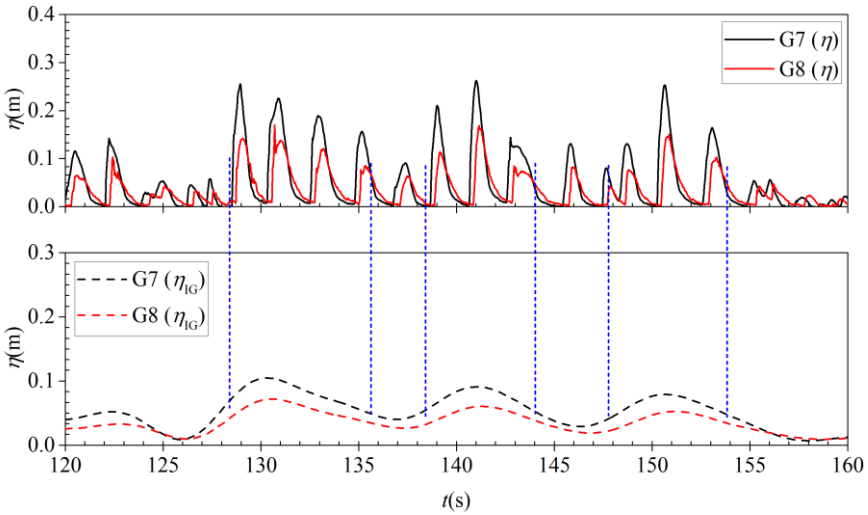

Fig. 8 Wave surface elevations at G7 and G8 for platform reef (h_r = 0.00 m, T_s = 2.0 s, H_s = 0.2 m)

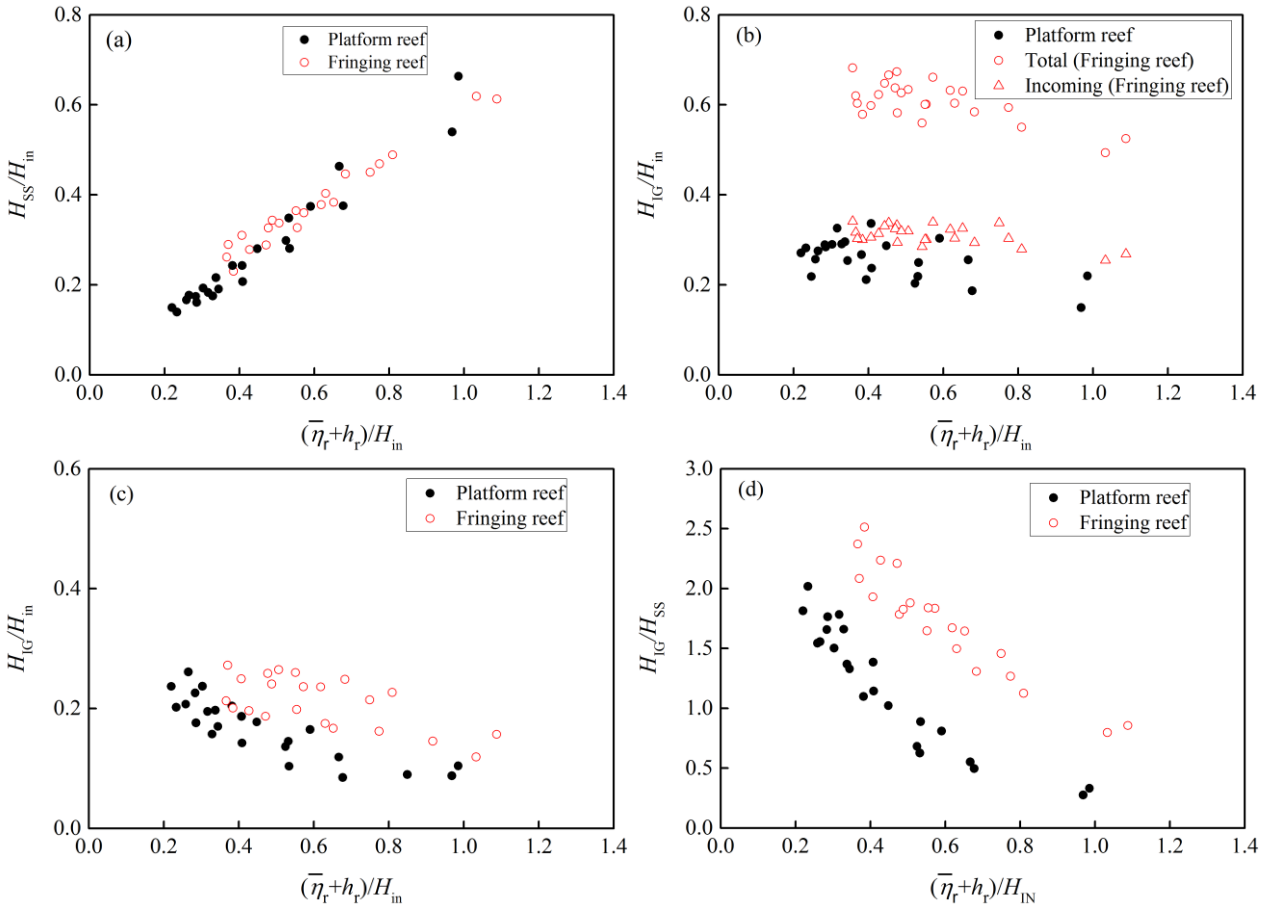

Fig. 9. Relationship between wave height and non-dimensional submergence depth on the reef flat. (a) Relative SS wave height H_{SS}/H_{in} at G15; (b) Relative IG wave height H_{IG}/H_{in} at G15; (c) Relative IG wave height H_{IG}/H_{in} at G6; (d) Ratio of IG wave height and SS wave height H_{IG}/H_{SS} at G15.

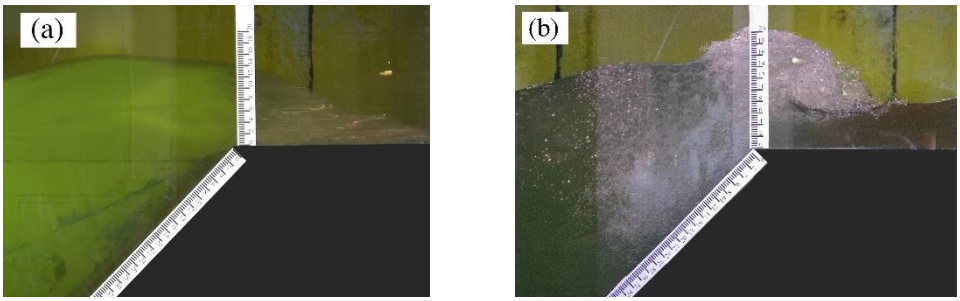

Fig. 10. Wave breaking around the reef edge. (a) Platform reef; (b) Fringing reef.

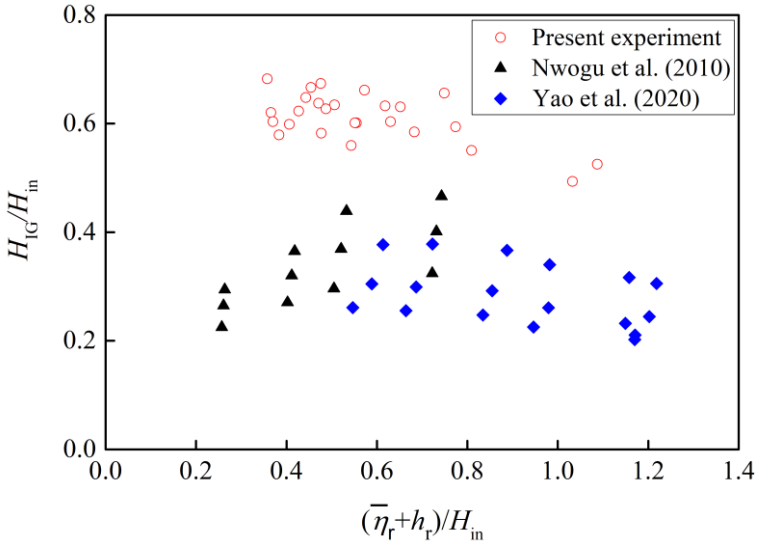

Fig. 11. Distribution of IG wave height for different larboratory experiments.

Table 1 Water depth on the reef flat and incident wave conditions

No.	Laboratory scale			Field scale		
	Water depth h_r (m)	Significant period T_s (s)	Significant wave height H_s (m)	Water depth h_r (m)	Significant period T_s (s)	Significant wave height H_s (m)
1	0	1.5	0.10	0	7.5	2.50
2	0	1.5	0.15	0	7.5	3.75
3	0	1.5	0.20	0	7.5	5.00
4	0	2.0	0.10	0	10	2.50
5	0	2.0	0.15	0	10	3.75
6	0	2.0	0.20	0	10	5.00
7	0.02	1.5	0.10	0.5	7.5	2.50
8	0.02	1.5	0.15	0.5	7.5	3.75
9	0.02	1.5	0.20	0.5	7.5	5.00
10	0.02	2.0	0.10	0.5	10	2.50
11	0.02	2.0	0.15	0.5	10	3.75
12	0.02	2.0	0.20	0.5	10	5.00
13	0.05	1.5	0.10	1.25	7.5	2.50
14	0.05	1.5	0.15	1.25	7.5	3.75
15	0.05	1.5	0.20	1.25	7.5	5.00
16	0.05	2.0	0.10	1.25	10	2.50
17	0.05	2.0	0.15	1.25	10	3.75
18	0.05	2.0	0.20	1.25	10	5.00
19	0.10	1.5	0.10	2.5	7.5	2.50
20	0.10	1.5	0.15	2.5	7.5	3.75
21	0.10	1.5	0.20	2.5	7.5	5.00
22	0.10	2.0	0.10	2.5	10	2.50
23	0.10	2.0	0.15	2.5	10	3.75
24	0.10	2.0	0.20	2.5	10	5.00

Table 2 Relative standard deviations at G15

Wave condition No.		RSD		
		$\bar{\eta}$	H_{SS}	H_{IG}
Platform reef	No. 6	0.011%	0.040%	0.068%
	No. 18	0.009%	0.205%	0.224%
	No. 24	0.012%	0.551%	0.483%
Fringing reef	No. 6	0.017%	0.072%	0.200%
	No. 18	0.008%	0.447%	0.627%
	No. 24	0.101%	0.720%	0.687%

Table A1 Infragravity wave heights in field observations and laboratory experiments

Article	Method	Reef	$H_{\mathrm{IG}}/H_{\mathrm{in}}$	Relationship between IG wave height and water depth
Pomeroy et al. (2012)	Field observation	Ningaloo Reef	0-0.14 (Mid Reef flat)	Proportional
Gawehn et al. (2016)	Field observation	Roi-Namur	0-0.4 (Inner Reef flat)	Proportional (Resonance)
Beetham et al. (2015)	Field observation	Funafuti Atoll	0.25 (Inner Reef flat)	Minimally affected by water depth
Nwogu and Demirbilek (2010)	Laboratory	Smooth surface Composite-slope reef face 1:12 shoreline	0.2-0.47 (Inner Reef flat)	Proportional (Resonance)
Yao et al. (2020)	Laboratory	Smooth surface 1:6 reef face 1:3.5 shoreline	0.15-0.38 (Inner Reef flat)	Inverse proportional
Present experiment	Laboratory	Smooth surface 1:1 reef face Vertical shoreline	0.49-0.68 (Inner Reef flat)	Inverse proportional